Design, Synthesis, Biology, and Conformations of Bicyclic α-Melanotropin Analogues

Carrie Haskell-Luevano,† Mark D. Shenderovich,† Shubh D. Sharma,† Gregory V. Nikiforovich,†,§ Mac E. Hadley,‡ and Victor J. Hruby*,†

Departments of Chemistry and Anatomy, University of Arizona, Tucson, Arizona 85721, and Center for Molecular Design, Washington University, St. Louis, Missouri 63130

Received November 2, 1994®

Seven side chain-constrained bicyclic α-melanotropin (α-MSH) analogues were designed and synthesized, their conformations analyzed, and their biological properties examined in the frog skin and lizard skin bioassays. The structure of these analogues is based on the central sequence Ac–Cys⁴-Xaa⁵-His⁶-DPhe⁷-Arg⁸-Trp⁹-Cys¹⁰-Lys¹¹-NH_2 (Xaa⁵ = Asp or Glu) and has been extended on the N-terminal with the amino acids Ser¹-Tyr²-Ser³ and on the C-terminal with Pro¹²-Val¹³ to more closely resemble the native hormone α-MSH. The analogue Ac-Cys⁴-Asp⁵-His⁶-DPhe⁷-Arg⁸-Trp⁹-Lys¹⁰-Cys¹¹-NH_2 also was synthesized, and its conformational and biological properties were examined. Design of these analogues was based upon the previously identified superpotent monocyclic peptides [Cys⁴,DPhe⁷,Cys¹⁰]α-MSH(4-10)-NH_2 and [Nle⁴,Asp⁵,DPhe⁷,Lys¹⁰]α-MSH(4-10)-NH_2 with the rationale of increasing conformational constraints to restrict the available backbone conformations as a means to identify the conformations that facilitate biological activity. Computer-assisted conformational analysis of the central tetrapeptide residues 6–9 identified β-turns which varied with respect to the residue in the $i + 1$ position. Each highly constrained peptide contains D-Phe⁷ and a 23-membered ring which has previously been identified as crucial to produce prolonged acting peptides with superagonistic activities. The bicyclic peptides reported in this study are full agonists and are 25-400-fold less potent than α-MSH in the frog and lizard skin bioassays.

Introduction

α-Melanocyte stimulating hormone (α-MSH, α-melanotropin) is a linear tridecapeptide consisting of the primary sequence Ac-Ser-Tyr-Ser-Met-Glu-His-Phe-Arg-Trp-Gly-Lys-Pro-Val-NH_2. This peptide hormone is generated by posttranslational processing of the preprohormone pro-opiomelanocortin (POMC).[1,2] The POMC gene has been identified as being expressed in the pituitary, brain, skin, testis, ovary, gastrointestinal tract, pancreas, placenta, lung, kidney, thyroid, and immune system.[3–6] Receptors for this hormone have been isolated in melanocytes, adrenal cortical cells, brain, gut, and other peripheral tissues.[7,8] Although α-MSH is most recognized for its role in melanin synthesis and dispersion in melanocytes involved in skin pigmentation,[9,10] it has also been implicated in possessing other central and peripheral biological activities such as learning, memory and attention,[11,12] analgesic effects,[13] modulation of body temperature,[14–16] role in fetal development and parturition,[17–21] and immunomodulatory effects.[22–24] Several different melanocortin receptor types have been isolated and cloned.[25–32] These were found to be expressed in several of the aforementioned tissues, and their diverse locations support the hypothesis of multiple peripheral and central biological activities.

α-MSH is a highly flexible linear peptide, and determination of its biologically relevant conformations required for receptor recognition and binding, signal transduction, and receptor dissociation has been difficult. Our approach, in overcoming the problem of an enormous number of allowed peptide backbone conformations and determining the biologically relevant ones, is the utilization of side chain to side chain cyclic constraints.[33,34] Several endeavors to "lock" in the bioactive conformations of α-MSH have been reported previously. These approaches have sought to stabilize a postulated reverse turn occurring in the active site region His-Phe-Arg-Trp. These side chain monocyclic analogues include Ac-[Cys⁴,Cys¹⁰]α-MSH-NH_2,[35] Ac-[Cys⁴,DPhe⁷,Cys¹⁰]α-MSH(4–11)-NH_2,[36] Ac-[Nle⁴,DOrn⁵,-Xaa⁷,Glu⁸]α-MSH(4–11)-NH_2 (where Xaa is L- or D-Phe),[37] Ac-[Nle⁴,Yaa⁵,DPhe⁷,Lys¹⁰]α-MSH(4–10)-NH_2 (where Yaa is Asp or Glu),[38,39] Ac-[Nle⁴,Asp⁵,DPhe⁷,-Zaa¹⁰,Lys¹¹]α-MSH(4–11)-NH_2 (where Zaa is Ala, Aib, or Sar),[40] and the N- to C-terminal monocyclic analogues cyclo(Gly-His-Xaa-Arg-Trp-Gly) (where Xaa is L- or D-Phe).[41] The cyclic disulfide Ac-[Cys⁴,Cys¹⁰]α-MSH-NH_2 and the cyclic lactam Ac-[Nle⁴,Asp⁵,DPhe⁷,Lys¹⁰]α-

* To whom reprint requests should be addressed at the Department of Chemistry.
† Department of Chemistry.
‡ Department of Anatomy.
§ Center for Molecular Design.
® Abstract published in *Advance ACS Abstracts,* April 15, 1995.

0022-2623/95/1838-1736$09.00/0

Table 1. Relative Potencies of Previously Reported Monocyclic and Linear α-MSH Analogues

peptide	structure	relative biological potencies: frog potency	frog EC_{50} (nM)	lizard potency	lizard EC_{50} (nM)
α-MSH	Ac-Ser-Tyr-Ser-Met-Glu-His-Phe-Arg-Trp-Gly-Lys-Pro-Val-NH_2	1.0(−)[a]	0.10	1.0(−)	1.0
	Ac-Cys-Glu-His-DPhe-Arg-Trp-Cys-Lys-NH_2	2.5[b](−)	0.04	3.0(−)	0.3
	Ac-NLe-Asp-His-DPhe-Arg-Trp-Lys-NH_2	0.8[c](+)	0.12	10−90.0(+)	0.01
	Ac-Nle-Asp-His-DPhe-Arg-Trp-Aib-Lys-NH_2	1.0[d](ND)	0.10	ND	ND
	Ac-Nle-DOrn-His-D-Phe-Glu-Trp-Gly-Lys-NH_2	0.001[e](−)	1000	inactive	
	cyclo(Gly-His-DPhe-Arg-Trp-Gly)	ND	1200[f]	ND	ND
	Ac-His-Phe-Arg-Trp-NH_2	0.000005[g](−)	30 000	0.0014[h](−)	15 000
	Ac-His-DPhe-Arg-Trp-NH_2	0.001[i](−)	150	0.1(−)	10
	Ac-DPhe-Arg-Trp-NH_2	0.00001[i](+)	10 000	0.001(+)	1000
	Ac-His-DPhe-Arg-NH_2	inactive[j]		inactive[j]	

[a] Indicates whether the peptide is prolonged (+) or not prolonged (−) acting. Literature references from [b]*Cody* et al.,[36] [c]*Al*-Obeidi et al.,[38] [d]*Nikiforovich* et al.,[40] [e]*Sugg* et al.,[37] [f]Bódi et al.,[41] [g]*Hruby* et al.,[52] [h]*Castrucci* et al.,[53] and [i]*Sawyer* et al.[57] [j] Showed no skin darkening at the concentrations examined (10^{-12}−10^{-5} M). ND = not determined.

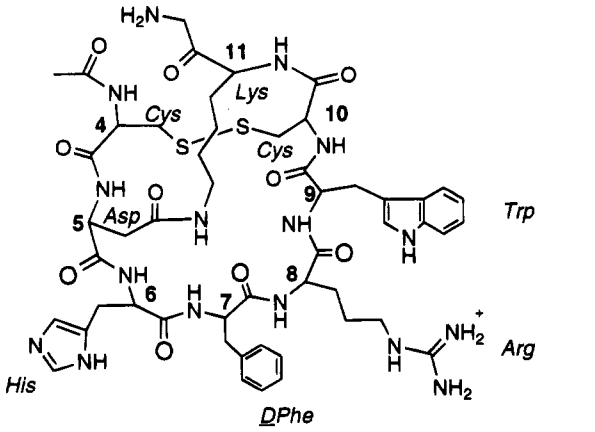

Figure 1. Structure of bicyclic analogue **VI**, Ac-Cys-Asp-His-DPhe-Arg-Trp-Cys-Lys-NH_2.

MSH(4−10)-NH_2 analogues were shown to be superpotent, prolonged acting analogues, whereas the other analogues generally were less potent than the native hormone (see Table 1 for biological activities of selected examples).

From these studies, we decided to further constrain α-MSH analogues by incorporating a second side chain to side chain covalent cycle, Figure 1. Upon examination of the biologial properties reported above, we decided to base our strategy on the monocyclic analogues Ac-[Cys^4,DPhe^7,Cys^{10}]α-MSH(4−10)-NH_2 and Ac-[Nle^4,Yaa^5,DPhe^7,Lys^{10}]α-MSH(4−10)-NH_2 (where Yaa is either Asp or Glu). The chimeric hybrids we designed and synthesized for this study all contained cysteine in the 4-position, glutamic or aspartic acid in the 5-position, D-phenylalanine in the 7-position, and cysteine and lysine in the 10- and 11-positions, respectively. One exception to the latter is analogue **VII** with lysine and cysteine in the 10- and 11-positions, respectively (Table 2). On the basis of Ac-[Cys^4,Cys^{10}]α-MSH compounds, the second side chain constraint was postulated both on the basis of molecular modeling studies which suggested the close spatial proximity of side chain functionalities Glu^5 and Lys^{11} [42] and on the relatively high potency of previous analogues with the lactam bridge between Asp^5 and Lys^{11}.[40] Although this bicyclization approach apparently has not been widely practiced with peptide hormones, it has been successful in converting a weak oxytocin agonist into a potent antagonist[43] and a potent somatostatin agonist to one with a long duration of action.[44,45] The overall aim of this study was to further limit the number of available backbone conformations centered around the "message" sequence His-DPhe-Arg-Trp in order to identify the biologically relevant backbone conformations of α-MSH analogues. This conformational information may also provide insight into the design of melanotropin peptidomimetics and nonpeptide derivatives. Computer-assisted conformational analysis of the peptides designed in this study identified four possible families of backbone conformations all consisting of a reverse turn with varying residues in the $i + 1$ position. We also added both N- and C-terminal amino acids, to the central common region of 4−11 residues, so as to more closely resemble the parent hormone α-MSH and examine the effect on biological potency that these residues have.

Results

Chemical Synthesis and Characterization. The partially protected peptide precursors were assembled on a low-substituted (0.37 mmol of NH_2/g) *p*-methylbenzhydrylamine (pMBHA) resin. Orthogonal solid-phase methodology was utilized to enable the formation of the lactam side chain monocycle while the peptide precursor was still attached to the resin (Scheme 1).[46] Briefly, *tert*-butyloxycarbonyl (Boc) was used for N^{α} protection and was removed with trifluoroacetic acid (TFA) in the presence of anisole. Most coupling reactions employed 1,3-diisopropylcarbodiimide (DIC) and *N*-hydroxybenzotriazole (HOBT) with the exception of the amino acids possessing fluorenylmethyloxycarbonyl (Fmoc) or fluorenylmethyl ester (OFm) side chain protecting groups. In these cases, (benzotriazolyloxy)-tris(dimethylamino)phosphonium (BOP) in *N*-methylpyrrolidinone (NMP) in the presence of diisopropylethylamine (DIEA) was employed as coupling reagent. Amino acid coupling times were 2 h and were monitored by the Kaiser test.[47] After TFA deprotection, resin washes included dichloromethane (DCM), DIEA (10% in DCM) for neutralization of the amino salt, and DCM. At the appropriate stage of synthesis (Scheme 1; see the Experimental Section), lactam cyclization was com-

Table 2. Comparative Biological Activities of Bicyclic α-MSH Analogues in the Frog Skin Bioassay

peptide	structure	relative peptide frog activity	
		relative potency[a]	EC_{50} (nM)
α-MSH	Ac-Ser-Tyr-Ser-Met-Glu-His-Phe-Arg-Trp-Gly-Lys-Pro-Val-NH_2	1.00(−)[b]	0.1
I	Ac-Ser-Tyr-Ser-Cys-Glu-His-DPhe-Arg-Trp-Cys-Lys-Pro-Val-NH_2	0.008(+)	12.5
II	Ac-Cys-Glu-His-DPhe-Arg-Trp-Cys-Lys-Pro-Val-NH_2	0.035(+)	3.0
III	Ac-Cys-Glu-His-D-Phe-Arg-Trp-Cys-Lys-NH_2	0.0035(−)	28.0
IV	Ac-Ser-Tyr-Ser-Cys-Asp-His-DPhe-Arg-Trp-Cys-Lys-Pro-Val-NH_2	0.007(+)	14.0
V	Ac-Cys-Asp-His-DPhe-Arg-Trp-Cys-Lys-Pro-Val-NH_2	0.04(+)	2.5
VI	Ac-Cys-Asp-His-DPhe-Arg-Trp-Cys-Lys-NH_2	0.018(±)	6.0
VII	Ac-Cys-Asp-His-DPhe-Arg-Trp-Lys-Cys-NH_2	0.003(+)	33.0

[a] All peptide activities were tested at a range of concentrations and compared to the half-maximal effective dose of α-MSH in the frog skin (10^{-10} M) bioassays. [b] Indicates that the response is superprolonged (+), prolonged (±), or not prolonged (−).

Scheme 1

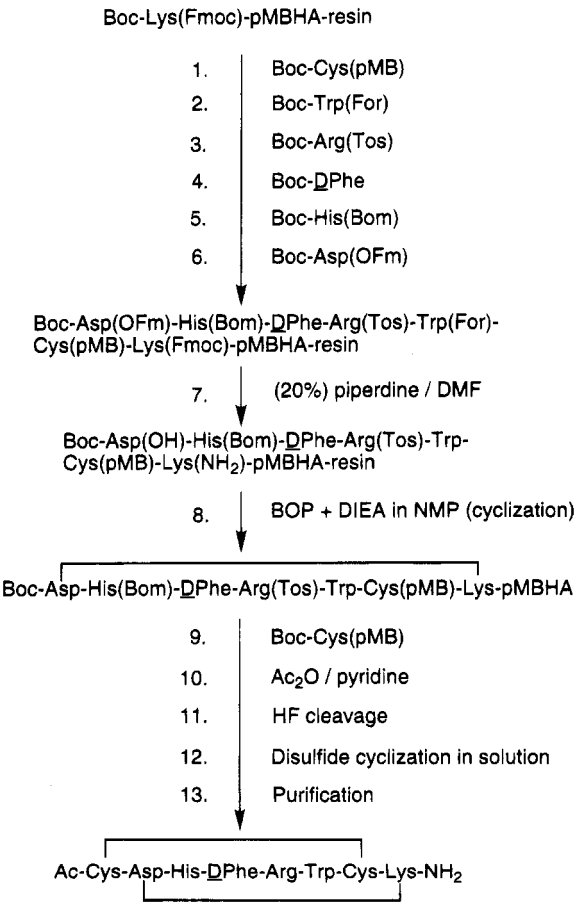

pleted using BOP and DIEA in NMP as coupling reagents. The coupling times of the cyclic lactam formation varied from 2 h to overnight and were repeated several times until a negative Kaiser test resulted. N-terminal acetylation was performed using acetic anhyride and pyridine in DCM. Following acetylation of the peptide precursor, the monocyclic conjugates were cleaved from the resin, along with the remaining side chain protecting groups, at 0 °C, in anhydrous HF. The crude peptides were isolated (see the Experimental Section), and the disulfide cyclization was performed in solution as described in the Experimental Section. Purification of these analogues was performed by reversed-phase high-pressure liquid chromatography (RP-HPLC). The purity of these peptides was assessed by fast atom bombardment mass spectrometry (FAB-MS), RP-HPLC, thin-layer chromatography (TLC) in three solvent systems, optical rotation, and amino acid analysis (see the Experimental Section).

Biological Evaluation. The melanotropic peripheral biological activities for the seven bicyclic analogues are summarized in Tables 2 and 3. The relative potencies and the EC_{50} values, compared to α-MSH, are given for both the frog and lizard skin bioassays. Prolongation, or residual activity, for these assays also is summarized and defined as (a) not prolonged if the assay skin darkening is less than 50% of the maximal response 60 min after the melanotropin has been removed from the incubation medium, (b) prolonged if the assay skin darkening remains greater than 50% of the maximal response 60 min after the melanotropin has been removed from the incubation medium, or (c) superprolonged if the assay skin darkening remains greater than 90% of the maximal response for longer than 60 min after the melanotropin has been removed from the incubation medium, Figure 2.

Evaluation of the bicyclic analogues in the frog skin bioassay, Table 2 and Figure 3, shows a variance in biological activities. The bicyclic analogues **I** and **IV**, which possess the 1−13 sequence, exhibit a 125−140-fold lower potency compared to α-MSH in the frog skin assay. Upon removal of the N-terminal residues Ser-Tyr-Ser (analogues **II** and **V**), a 4−6-fold increase in potency is observed compared to the respective 1−13 analogues. Analogues **III** and **VI**, which have undergone both N- and C-terminal truncation to consist only of residues 4−11, have decreased biological potency of 60−280-fold compared to α-MSH and a 10-fold decrease compared to the 4−13 sequence. Analogue **III** possessed approximately a 2-fold decrease in potency compared to its respective 1−13 analogue (**I**). The latter 2-fold decrease is within experimental error of the frog skin bioassay, which is generally ±3-fold, due primarily to seasonal animal variation. Therefore, peptide **III** is approximately equipotent to analogue **I**. Analogues

Table 3. Comparative Biological Activities of Bicyclic α-MSH Analogues in the Lizard Skin Bioassay

peptide	structure	relative peptide lizard activity: relative potency[a]	relative peptide lizard activity: EC_{50} (nM)
α-MSH	Ac-Ser-Tyr-Ser-Met-Glu-His-Phe-Arg-Trp-Gly-Lys-Pro-Val-NH_2	1.00(−)[b]	1.0
I	Ac-Ser-Tyr-Ser-Cys-Glu-His-DPhe-Arg-Trp-Cys-Lys-Pro-Val-NH_2	0.03(±)	33.0
II	Ac-Cys-Glu-His-DPhe-Arg-Trp-Cys-Lys-Pro-Val-NH_2	0.03(+)	33.0
III	Ac-Cys-Glu-His-DPhe-Arg-Trp-Cys-Lys-NH_2	0.0025(±)	400
IV	Ac-Ser-Tyr-Ser-Cys-Asp-His-DPhe-Arg-Trp-Cys-Lys-Pro-Val-NH_2	0.03(±)	33.0
V	Ac-Cys-Asp-His-DPhe-Arg-Trp-Cys-Lys-Pro-Val-NH_2	0.03(±)	33.0
VI	Ac-Cys-Asp-His-DPhe-Arg-Trp-Cys-Lys-NH_2	0.03(±)	33.0
VII	Ac-Cys-Asp-His-DPhe-Arg-Trp-Lys-Cys-NH_2	0.03(±)	33.0

[a] All peptide activities were tested at a range of concentrations and compared to the half-maximal effective dose of α-MSH in the lizard skin (10^{-9} M) bioassays. [b] Indicates that the response is superprolonged (+), prolonged (±), or not prolonged (−).

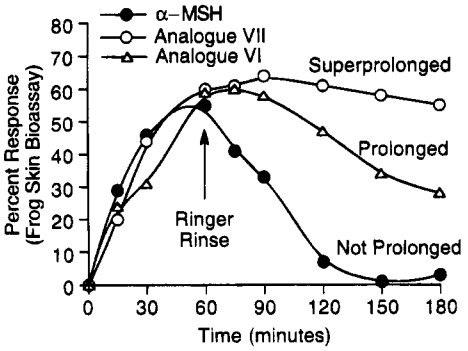

Figure 2. Demonstration of the superprolonged effect of the bicyclic analogue Ac-Cys-Asp-His-DPhe-Arg-Trp-Lys-Cys-NH_2 in the frog skin bioassay system, the prolongation effect of Ac-Cys-Asp-His-DPhe-Arg-Trp-Cys-Lys-NH_2, and the not prolonged effect of α-MSH in the same assay.

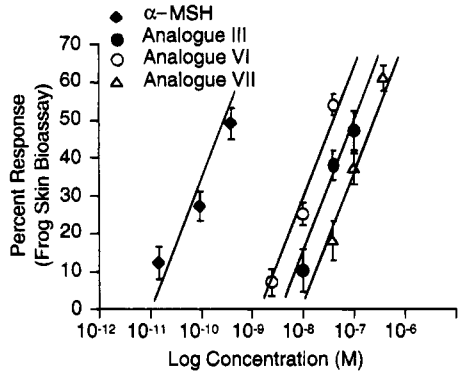

Figure 3. Comparison of the frog skin biological potencies of the bicyclic analogues shown in Table 2. Each value represents the mean darkening response of skins (N = 5) to the melanotropins at the concentration noted.

IV–**VII** have had Glu^5 replaced by Asp. Removal of a methylene side chain moiety demonstrated no significant alteration in biological potency when comparing the 1–13 and 4–13 compounds containing the naturally occurring glutamic acid. Interestingly, the substitution of Asp^5 (analogue **VI**) for Glu^5 (analogue **III**) in the 4–11 sequence resulted in a 5-fold decrease in potency, relative to each other. This small difference falls outside

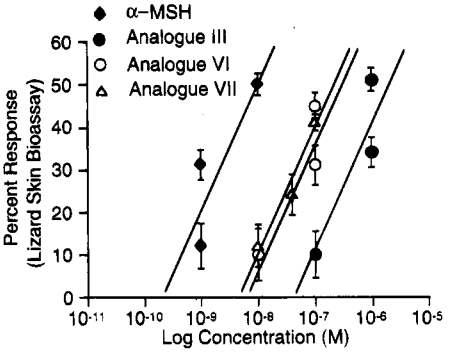

Figure 4. Comparison of lizard skin biological potencies of the bicyclic analogues shown in Table 3. Each value represents the mean darkening response of skins (N = 5) to the melanotropins at the concentration noted.

of the experimental error, suggesting that the subtle difference between the conformations of these two analogues may be biologically relevant and hinting at refined ligand–receptor interactions. Analogue **VII**, where the 23-membered cycle incorporated a lactam bridge between residues Asp^5 and Lys^{11} versus the Cys^4,Cys^{10} disulfide bridge for analogues **I**–**VI**, shows a 333-fold decrease in potency compared to α-MSH and approximately a 6-fold decrease in potency compared to its counterpart, analogue **VI**. Once again, subtle differences in biological potency are observed.

In the lizard skin bioassay, Table 3 and Figure 4, all of these bicyclic compounds demonstrated a 33-fold decrease in potency compared to α-MSH, and all are nearly equipotent to each other with the exception of analogue **III** which is 400-fold less potent than α-MSH and 12-fold less active than the other bicyclic analogues. Melanoma tyrosinase activity for analogues **V**–**VII** demonstrates a 10–100-fold decrease in the minimal effective dose compared to that for α-MSH (data not shown). In this bioassay, analogues **VI** and **VII** appear to possess equipotent activities in agreement with the lizard skin assay.

Energy Calculations. The starting sequences for the buildup procedures used in energy calculations for bicyclic analogues **III**, **VI**, and **VII** are outlined in Table 4. Monocyclic (MC) precursors of the bicyclic analogues **III**, **VI**, and **VII** (denoted as MC-**III**, MC-**VI**, and MC-

Table 4. Buildup Procedures Used in Energy Calculations of Bicyclic α-MSH Analogues

analogue	step	sequence considered	no. of conformers considered	no. of conformers selected	ΔE (kcal/mol)	distance constraint (Å)
MC-**VI**	1	Ac-Asp-His-DPhe-Arg-Trp-Ala-Lys-NH_2	22	9	12	$C^{\alpha}_4-C^{\beta}_{10} \leq 8.0$
	2	Ac-Ala-Asp-His-DPhe-Arg-Trp-Ala-Lys-NH_2	51	26	10	$C^{\beta}_4-C^{\beta}_{10} \leq 4.0$
VI	3	Ac-Cys-Asp-His-DPhe-Arg-Trp-Cys-Lys-NH_2	26	19	10	
MC-**III**	1	Ac-Cys-Abu-His-DPhe-Arg-Trp-Cys-Abu-NH_2	26	22	10	$C^{\gamma}_5-C^{\gamma}_{11} \leq 6.0$
III	2	Ac-Cys-Glu-His-DPhe-Arg-Trp-Cys-Lys-NH_2	22	17	10	
MC-**VII**	1	Ac-Asp-His-DPhe-Arg-Trp-Lys-NH_2	64	28	10	$C^{\alpha}_4-C^{\alpha}_{11} \leq 9.0$
	2	Ac-Ala-Asp-His-DPhe-Arg-Trp-Lys-Ala-NH_2	1008	136	10	$C^{\beta}_4-C^{\beta}_{11} \leq 4.0$
VII	3	Ac-Cys-Asp-His-DPhe-Arg-Trp-Lys-Cys-NH_2	136	82	10	

VII in Table 4) were considered in previous studies.[40,48,49] Unfortunately, the buildup procedures and the cyclization templates for both analogues **III** and **VI** were identical, thus giving identical conformational families for these analogues, as seen in Table 4. Due to these limitations of theory, analogue **III** was removed from any further discussion describing the energy calculations. Low-energy conformers ($\Delta E \leq 10$ kcal/mol) obtained for these monocyclic analogues, MC-**VI** and MC-**VII**, were used as templates to build up the disulfide cycle. In previous studies[40,48,49] only the first step of lactam bridge closure was completed and did not always result in correct valence geometry for the Asp C^{δ}–Lys N^{ϵ} moiety. Therefore, we first refined the conformations of Ac-Asp-His-DPhe-Arg-Trp-Ala-Lys-NH_2 (MC-**VI**) and Ac-Asp-His-DPhe-Arg-Trp-Lys-NH_2 (MC-**VII**), Table 4, by additional energy minimization employing a second mode of lactam bridge closure (described in the Experimental Section). Both energy and distance cutoff criteria were applied, as shown in Table 4, in order to select those conformers which would allow disulfide bridge formation.

The disulfide bridge closure for analogues **VI** and **VII** were accomplished in two steps. First, blocked Ala residues were added at the N-terminus of MC-**VI**, Ac-Ala-Asp-His-DPhe-Arg-Trp-Ala-Lys-NH_2, and at both termini of MC-**VII**, Ac-Ala-Asp-His-DPhe-Arg-Trp-Lys-Ala-NH_2 (see step 2 in Table 4). For analogue **VI**, three starting conformations of Ala^{11} (ϕ,ψ = −150°,150°; −80°,80°; 60°,60°) and three values of Lys^{10} ψ angle, −40°, 150°, and 60° (only the latter being allowed when ϕ was positive), were also considered, and the number of starting conformations was reduced before minimization by examining the $C^{\beta}_4-C^{\beta}_{11}$ distance. For analogue **VII**, three starting conformations of Ala^4 (ϕ,ψ = −150°, 150°; −80°,80°; −70°,−40°) and two or three values of the Asp^5 ϕ angle, −150°, −80°, and 60° (the latter being allowed only when ψ was positive), were combined with the selected lactam bridge conformers of MC-**VI**. Energy minimization at these stages included a one-side penalty potential (see the Experimental Section) with the force constant of U_o = 10 kcal/mol Å^2 which was applied when the distance between C^{β}_4 and C^{β}_{10} of analogue **VI** and C^{β}_4 and C^{β}_{11} of analogue **VII** exceeded the distance constant of d_o = 4.0 Å. Final energy minimization included the complete set of disulfide and lactam cycle closure potentials (described in the Experimental Section). Optimal starting values of cysteine χ^1 angles were selected by an algorithm described in previous studies.[50]

The final sets of low-energy conformers of the bicyclic analogues **VI** and **VII** were classified according to the backbone conformational code of Zimmerman and Scheraga[51] and by χ^1 rotamers of side chains in positions 4, 5, 10, and 11 involved in a cycle formation. The conformers which have the same backbone conformational code and the same χ^1 rotamers were assumed to be similar. The lowest energy conformers were selected to represent such groups of similar conformers. Within the energy cutoff ΔE = 10 kcal/mol, 19 and 82 conformers were selected for analogues **VI** and **VII**, respectively.

Discussion

We have designed side chain to side chain bicyclic peptide analogues of α-melanotropin to limit the number of available backbone conformations and to try and identify the bioactive conformations of α-MSH derivatives. This information may also be used in the design of melanotropin mimetics. These studies were based upon the creation of hybrids between two highly potent monocyclic compounds, Ac-[Cys^4,DPhe^7,Cys^{10}]α-MSH(4–11)-NH_2[35,36] and Ac-[Nle^4,Asp^5,DPhe^7,Lys^{10}]α-MSH(4–10)-NH_2.[38,39] Molecular modeling studies of various peptide lengths of Ac-[Cys^4,Cys^{10}]α-MSH analogues by some authors[42] suggested that one of the possible bioactive conformational clusters brings the Glu^5 and Lys^{11} side chain moieties within the correct special proximity to allow the formation of a salt bridge, the possibility of creating a covalent bond between the two, and predicting the design of bicyclic analogues possessing superpotent biological activities. Several factors were taken into consideration for the design of the peptide analogues presented in this study. The 23-membered ring, in addition to the D-Phe^7 replacement, is important for biological potency. By creating a second side chain to side chain cycle, perhaps the "ideal" biological conformation needed for molecular recognition of the receptor could be trapped, and a superagonist, with multiple constraints and a limited number of available conformations, would result. Alternatively bicyclization could "trap" the analogues in a poor biological conformation. To try and maximize our

chances for success, we chose the more flexible [Cys⁴,Cys¹⁰] disulfide bridge to represent the 23-membered ring and used Glu⁵ and Lys¹¹ to form the more rigid second bridge by lactam cyclization (27-membered ring). The second bridge also was decreased to a 26-membered ring with the replacement of Glu⁵ by Asp⁵. This modification was based upon the previous observations of Ac-[Nle⁴,Asp⁵,DPhe⁷,Zaa¹⁰,Lys¹¹]α-MSH-(4–11)-NH_2 (where Zaa is Ala or Aib) analogues which were reported to possess relatively high potencies in the frog skin bioassay.[40] The 1–13, 4–13, and 4–11 analogues were synthesized to identify which of these three sequence chain lengths is the minimum one needed while retaining the desired biological properties that can be used in structural modifications and to reexplore the role of the amino acid residues 1–3, 12, and 13 on biological potencies. Having determined the minimum amino acid sequence in the lizard skin assay needed for analogues containing Asp⁵ as the 4–11 sequence, we decided to see what biological effect would result upon changing the more flexible [Cys⁴,Cys¹⁰] disulfide (23-membered ring) to an even more flexible [Cys⁴,Cys¹¹] (26-membered ring)-containing analogue and having the more rigid [Asp⁵,Lys¹⁰] lactam bridge becoming the predominant 23-membered ring. This alteration (**VII**, Table 2) led to a 6-fold decreased potency in the frog skin assay, as compared to analogue **VI**. However, the relative potency in the lizard assay was not affected by this modification (Table 3). The surprising finding of almost identical biological potencies in the lizard skin bioassay demonstrates that whatever conformational differences exist between the various chain lengths (Asp⁵ or Glu⁵ residues), or changes in the flexibility of the 23-membered ring, are not important in this assay system. The frog skin bioassay, however, can detect these small conformation distinctions as demonstrated by the 5.5-fold range of relative potencies between the bicyclic analogues, Figure 3. Completion of synthesis and biological evaluations of analogues **I**–**VII** (Tables 2 and 3) demonstrates that, while maintaining full agonistic nanomolar biological potencies, these compounds are not equipotent or superpotent compared to the parent hormone α-MSH.

Several interesting results have been revealed by this study. The first intriguing observation is that in analogues **I** and **IV**, which contain the 1–13 sequence, deletion of the first three N-terminal residues, Ser-Tyr-Ser, leads to a decrease in potency in the frog bioassay as compared to their 4–13 counterparts, analogues **II** and **V**, respectively. Previous studies examining the minimal α-MSH sequence required for biological activity in both the frog and lizard skin bioassays determined that the first three N-terminal residues contribute minimally or not at all to biological potency.[52–54] In all studies involving these assays that were previously reported, no where had it been found that by the addition of these residues a loss in potency occurs. With these compounds, however, the dual conformational constraints introduced by the formation of the two side chain to side chain cycles can affect the side chain topology (χ space) in addition to the backbone φ,ψ space. These steric effects may modify the topographical presentation of these residues in a manner that is energetically unfavorable for maximum interaction with the receptor. Residues Pro¹² and Val¹³ appear to maintain the potentiating effect previously observed in the frog skin bioassay.[52,55]

Surprisingly, the presence of the Ser-Tyr-Ser N-terminal residues and the C-terminal residues Pro and Val had no potentiating effect on the biological activities of these bicyclic compounds in the lizard bioassay. These residues have been previously identified as potentiating residues for linear melanotropins in the lizard skin bioassay with Pro¹² playing a particularly important role in increasing ligand potency.[53] These observations would suggest that the ligand–receptor interaction is occurring with the central common sequence His-DPhe-Arg-Trp, with the side chain bicyclics orientating these key residues in a similar topographical presentation to the receptor for all the bicyclic analogues presented here. When examining the lizard skin activities, there was no change in biological potency relative to α-MSH and each other, except for analogue **III** which exhibited a 12-fold decrease in potency relative to the other bicyclic peptides. This unexpected finding may suggest that the Pro¹² and Val¹³ amino acid residues maintain the potentiating effects that are consistent with previous studies on linear melanotropins.[53] It is interesting, however, that this potentiating effect of the Pro¹² and Val¹³ residues is not seen in the other 4–11 analogues (**VI** and **VII**) which maintain equipotency with the 1–13 and 4–13 analogues. These particular residues are located outside the cyclic constraints and the proposed message sequence, His-DPhe-Arg-Trp, which presumably maintains the same topographical presentation to the receptor for all the analogues possessing equipotent biological activity. We can speculate that for analogue **III** the side chains of Pro¹² and/or Val¹³ may interact sterically with one or both side chain cycles in a manner that changes the side chain orientation and/or the backbone conformations of the central 6–9 residues producing a less favorable ligand–receptor interaction accounting for the drop in potency. Analogue **III** differs from the other two 4–11 compounds by having a Glu in position 5 instead of Asp. This modification causes the lactam cycle to consist of a slightly more flexible 27-membered ring instead of the 26-membered ring present in analogues **VI** and **VII**. This subtle difference may support the speculation that the side chain cycles affect available backbone conformations and possibly side chain topology.

The biological activities of the bicyclic analogues presented in Tables 2 and 3 and Figures 3 and 4 show different biological profiles for the frog and lizard skin bioassays. The frog skin assay demonstrates a range in potencies, while in the lizard skin assay, all analogues are nearly equipotent, with the exception of analogue **III**. This observation between bioassay systems is not unique to the compounds examined in the study. Generally, our laboratories have observed that the lizard skin bioassay has yielded results with more tightly grouped dose–response curves, whereas the frog bioassay system produces relative potencies that cover a wider range of ligand dose–response concentrations.[56] This phenomena can be attributed to different melanotropin receptor subtypes, with the frog bioassay system apparently being more sensitive to subtle conforma-

tional and structural differences. The biological results shown in Table 2 and Figure 3 are a good example demonstrating a range of potencies in the frog skin bioassay, while the same analogues possess approximately the same biological potencies in the lizard skin bioassay (with the exception of compound **III**), Table 3 and Figure 4. The lizard assay system, however, has been observed to have similar structure–activity relationships as mammalian melanoma data and, hence, is considered to more closely resemble the mammalian system.[56]

Previous studies have identified the central residues His^6-Phe^7-Arg^8-Trp^9 as being the minimal active α-MSH sequence eliciting a full biological response in both the frog and lizard skin bioassays.[52,53] In the frog bioassay, this core sequence was reported to have a relative potency of 0.000005 compared to α-MSH, which corresponds to an EC_{50} value of approximately 30 μM.[52] In the lizard bioassay system, the same peptide had a relative potency of 0.001, compared to α-MSH, which corresponds to an approximate EC_{50} value of 15 μM (Table 1).[53] Further studies replacing the naturally occurring L-Phe^7 by D-Phe^7 in the tetrapeptide Ac-His-DPhe-Arg-Trp-NH_2 lead to relative potencies and EC_{50} values of 0.001 and 150 nM in the frog assay system and 0.1 and 10 nM in the lizard skin assay system (Table 1).[57] This latter sequence, His^6-DPhe^7-Arg^8-Trp^9, is the same as the central sequence of all of the bicyclic analogues prepared in this study. Comparison of this tetrapeptide in the frog skin assay with the bicyclic analogues shows the bicyclic analogues to possess considerably greater potency, between 3- and 40-fold, than the tetrapeptide (compare Tables 1–3). Examination and comparison of this same tetrapeptide with the bicyclic analogues in the lizard skin bioassay, however, show the tetrapeptide possesses a 3-fold greater potency than most of the bicyclic analogues, except for **III** which is 40 times less potent. This comparison suggests that the flexible linear tetrapeptide can assume a conformation that is quite compatible with the requirement for the receptor in the lizard skin system, compared to the bicyclic analogues, whereas of all the possible conformations available to the linear peptide, none is more compatible with the requirements for the receptor in the frog skin assay system than that available to the bicyclic analogues. These comparisons pose an interesting problem in the design and evaluation of α-MSH analogues for further structure–function studies. As discussed previously, the differences in the two bioassay systems are prominent here. The observation that the tetrapeptide Ac-His-DPhe-Arg-Trp-NH_2 is less potent than the bicyclic analogues in the frog skin assay system, but more potent in the lizard skin assay, poses an intriguing problem. The question becomes on which assay system do we base further conformational structure–biological activity studies? Our solution to this observation, in terms of trying to identify the bioactive conformations of melanotropins in the mammalian system, is to suggest that the biological potencies in the lizard assay are more relevant than those of the frog assay system as previously discussed (*vide supra*).[56] Binding and cAMP studies performed on human melanocyte peripheral melanocortin receptors also suggest that the lizard skin bioassay results may more closely resemble the mammalian system than do the frog skin bioassay results.[26,58]

Comparison of the bicyclic analogues with the original monocyclic analogues in both bioassays shows that the bicyclic compounds are less potent than the monocyclic parents, Table 1. Thus the constrained conformations of the bicyclic analogues used here are unable to obtain the superagonist conformations available to the more flexible linear monocyclics or that predicted from previous modeling studies.[42] Nonetheless they still share all the necessary stereostructural and dynamic properties necessary for receptor recognition and signal transduction. Since the results from the lizard assay system appear to be more relevant to the mammalian system, the available conformations of the bicyclic analogues need to be examined. Upon further scrutiny of Table 3, we decided to proceed with the two bicyclic analogues consisting of the 4–11 sequence (**VI** and **VII**), since these compounds are comprised of a smaller number of residues and demonstrated approximately the same biological potencies. Analogue **III**, which possesses 12-fold decreased potency compared to analogues **VI** and **VII**, has been omitted from these comparisons as a result of the findings of the theoretical procedures used in this study (see the Energy Calculations subsection).

Classification and Comparison of Conformers. Comprehensive studies support the tetrapeptide sequence His^6-DPhe^7-Arg^8-Trp^9 as the "message" sequence of D-Phe^7-containing analogues of α-MSH. We therefore focused our conformational study on a comparison of the three-dimensional structure of this tetrapeptide in the ring system of two bicyclic analogues **VI** and **VII** between themselves and with the previously proposed models of the bioactive conformations for [DPhe^7]α-MSH,[48] [Cys^4,Cys^{10}]α-MSH(4–10)-NH_2,[42] and Ac-[Nle^4,Asp^5,DPhe^7,Lys^{10}]α-MSH(4–10)-NH_2.[49] These comparisons were made between the C^α and C^β carbons of the four residues His^6-DPhe^7-Arg^8-Trp^9 and the same atoms in the tripeptide regions His^6-DPhe^7-Arg^8 or DPhe^7-Arg^8-Trp^9. Buildup procedures, summarized in Table 4, ensured selection of representative sets of backbone conformations in the tetrapeptide region 6–9 of the bicyclic analogues. A systematic search for all sterically allowed rotamers of the side chains in positions 6–9 was not performed. We therefore chose the C^α atoms of residues 5–10 and the C^β atoms of residues 6–9 to represent, respectively, backbone and side chains of the central tetrapeptide in best fit matching of the conformers under study.

Matching and cluster analysis performed on analogue **VI** revealed four clusters of conformers with root mean square (rms) deviations less than 0.7 Å. The lowest energy conformers represented in each cluster are included in Table 5. These conformers possess three different locations of a β-turn: a type III β-turn centered at residues Arg^8-Trp^9 (conformers 1 and 2 in Table 5), a type II′ β-turn at DPhe^7-Arg^8 (conformer 3), and a type II β-turn centered at His^6-DPhe^7 (conformer 4). Each type of β-turn is stabilized by one or two transannular hydrogen bonds.

Sets of sterically allowed conformers for the central tetrapeptide (residues 6–9) of analogue **VII** appeared to be more diverse than those of analogue **VI**. Interestingly, the 23-membered lactam ring from this analogue

Table 5. Backbone Torsion Angles (deg) of Selected Low-Energy Conformers of the Bicyclic Analogues of α-MSH

amino acid residues	torsion angles	analogue **VI**				analogue **VII**			
		1	2	3	4	1	2	3	4
Cys^4	ϕ	−159	−74	−86	−105	−83	−62	−73	−158
	ψ	167	−39	81	122	−51	119	−36	144
Asp^5	ϕ	−160	−75	−105	−85	−167	−154	−66	−172
	ψ	43	87	9	147	157	154	99	137
His^6	ϕ	−113	−89	−132	−70	59	−87	−98	−141
	ψ	25	−16	30	98	29	−19	57	43
D-Phe^7	ϕ	157	152	68	96	62	−47	91	62
	ψ	−165	−138	−107	24	28	−61	−127	−107
Arg^8	ϕ	−73	−75	−64	−151	−139	−101	−85	−56
	ψ	−31	−14	−37	150	150	−3	−16	−41
Trp^9	ϕ	−71	−56	−89	−60	−88	58	−78	−94
	ψ	−23	−44	139	153	65	76	110	74
Cys^{10}	ϕ	−86	−87	−132	−74	−89	−139	−115	−76
(Lys^{10})	ψ	−55	−51	158	157	−8	42	73	85
Lys^{11}	ϕ	−86	−89	−81	−80	−80	−98	52	−57
(Cys^{11})	ψ	69	67	74	76	77	141	48	136
ΔE (kcal/mol)		0.0	0.4	0.4	1.5	0.0	4.2	4.4	4.6

Table 6. Backbone Torsion Angles (deg) of the Biologically Active Conformations in Previously Reported Models for α-MSH Analogues

peptide model	Asp/Glu^5		His^6		L/D-Phe^7		Arg^8		Trp^9		Lys/Cys^{10}	
	φ	ψ	φ	ψ	φ	ψ	φ	ψ	φ	ψ	φ	ψ
[DPhe^7]α-MSH[a]	−84	−19	−66	110	114	−9	−116	−62	57	66	−140	161
Ac-[Nle^4,Asp^5,DPhe^7,Lys^{10}]α-MSH(4−10)-NH_2[b]	−56	−59	−96	145	88	−65	−65	−58	−95	−56	−90	89
Ac-[Cys^4,Cys^{10}]α-MSH(4−10)-NH_2, model 1[c]	−136	158	−85	−29	−66	−37	−160	149	−53	−63	−164	152
Ac-[Cys^4,Cys^{10}]α-MSH(4−10)-NH_2, model 2[c]	−78	75	−70	−14	−53	−35	−109	−59	−162	149	−141	137

[a] Model preliminary reported by Sharma et al.[48] [b] Model preliminary reported by Sharma et al.[49] [c] Models reported by Nikiforovich et al.[42] refined by energy minimization using the ECEPP/2 force field.[60]

is theoretically more rigid than the 23-membered disulfide ring of analogue **VI**. Cluster analysis identified 15 clusters of structures with rms deviations less than 1.0 Å. The four conformational families most characteristic of these conformers are given in Table 5. These conformers represent different types of β-turns: a type III′ at His^6-DPhe^7 (the lowest energy conformer 1 in Table 5), two consecutive type I/III β-turns at residues 6, 7, and 8 (conformer 2), and a type II′ β-turn at DPhe^7-Arg^8 (conformers 3 and 4). In contrast to analogue **VI**, analogue **VII** has no conformer with a clearly defined β-turn centered at the residues Arg^8-Trp^9. This may rule out a reverse turn occurring at these residues.

The lowest energy conformers representing each of the 15 clusters found for analogue **VII** were selected for comparison with the four conformers of analogue **VI** according to the principles described above. The conformers 1−3 of analogue **VI** share close similarity with several conformers of analogue **VII** (rms ≤ 1.0 Å). The most similar conformers of the two analogues possess the type II′ β-turn at DPhe^7-Arg^8. This observation is in agreement with previous proposed models, and a D-configuration for the amino acid residue in the $i + 1$ position is thought to stabilize a β-turn.[56,59] Conformer 4 of analogue **VI** has a type II′ β-turn at positions 6 and 7 but does not display close similarity with any low-energy conformer of analogue **VII** (minimum rms = 1.3 Å). Similarly, conformers 1 and 2, as well as several other conformers of analogue **VII** containing a β-turn at residues His^6-DPhe^7, do not match any conformer of analogue **VI**. This allows us to disregard these conformations, since we are assuming that the same biological potency results from similar conformations.

The C^α and C^β carbons of residues His^6-DPhe^7-Arg^8-Trp^9 for the bicyclic analogues **VI** (conformers 1−4) and **VII** (conformers 3 and 4) were compared to the proposed biologically active conformations of [DPhe^7]α-MSH,[48] Ac-[Nle^4,Asp^5,DPhe^7,Lys^{10}]α-MSH(4−10)-NH_2,[49] and Ac-[Cys^4,Cys^{10}]α-MSH(4−10)-NH_2[42] (backbone torsion φ,ψ angles of the latter compounds are listed in Table 6). It was found that none of the representative low-energy conformers of analogues **VI** and **VII** matches the message tetrapeptide 6−9 of any of the previously reported models of biologically active conformations with rms values less than 1.0 Å. We therefore examined the tripeptide residue 6−8 and 7−9 C^α and C^β carbons for the "best fit". Table 7 summarizes the observations from this comparison. Both tripeptide sequences were examined, and the comparison listed in Table 7 is the tripeptide that was found to have the smallest rms deviation. These results enabled us to suggest that the preferred conformations of the highly constrained bicyclic analogues cannot exactly fit the receptor binding sites for all four "message" side chains (residues 6−9) of α-MSH or that the backbone restriction of residues 6−9 does not allow the bicyclic analogues to achieve the necessary dynamic receptor-bound superagonist conformations. On the other hand, several conformers of residues 6−8 or 7−9 in the bicyclic analogue display close C^α and C^β carbon matching to the proposed biologically active conformation of [DPhe^7]α-MSH and/or Ac-[Nle^4,Asp^5,DPhe^7,Lys^{10}]α-MSH(4−10)-NH_2. Both models have very similar arrangement of their His^6, DPhe^7, and Arg^8 residues, with rms values of 0.14 Å for the C^α and C^β atoms. The C^α and C^β atoms of residues 6−8 of the bicyclic analogue **VI** in conformation 4 almost exactly match the same carbon atoms of the [DPhe^7]α-

Table 7. Root Mean Square Deviations (Å) of C^{α} and C^{β} Atoms of Residues 6–9 in Low-Energy Conformers of Bicyclic Analogues of α-MSH and Models of Biologically Active Conformations of Linear and Monocyclic Analogues of α-MSH

	low-energy conformers of bicyclic analogues					
	analogue **VI**				analogue **VII**	
model[a]	1	2	3	4	3	4
[DPhe^7]α-MSH	1.91 (0.91)[c]	1.68 (0.73)[c]	1.52 (0.67)[b]	1.32 (0.19)[b]	1.84 (0.74)[b]	1.54 (0.65)[b]
Ac-[Nle^4,Asp^5,DPhe^7,Lys^{10}]α-MSH(4–10)-NH_2	1.68 (0.71)[c]	1.39 (0.74)[c]	1.10 (0.32)[c]	1.55 (0.28)[b]	1.45 (0.60)[b]	1.12 (0.30)[b]
Ac-[Cys^4,Cys^{10}]α-MSH(4–10)-NH_2, model1	1.20 (1.13)[b]	1.44 (0.95)[b]	1.67 (0.98)[b]	1.95 (0.94)[b]	1.45 (0.79)[b]	2.14 (1.02)[b]
Ac-[Cys^4,Cys^{10}]α-MSH(4–10)-NH_2, model 2	1.39 (0.88)[c]	1.19 (1.05)[b]	1.15 (0.78)[b]	2.12 (0.77)[b]	1.05 (0.80)[b]	1.20 (0.80)[b]

[a] See Table 6 for description of the peptide model's backbone torsion angles. [b,c] Lower values of RMS deviations of C^{α} and C^{β} atoms of tripeptides 6–8 (b) or 7–9 (c) are given in parentheses.

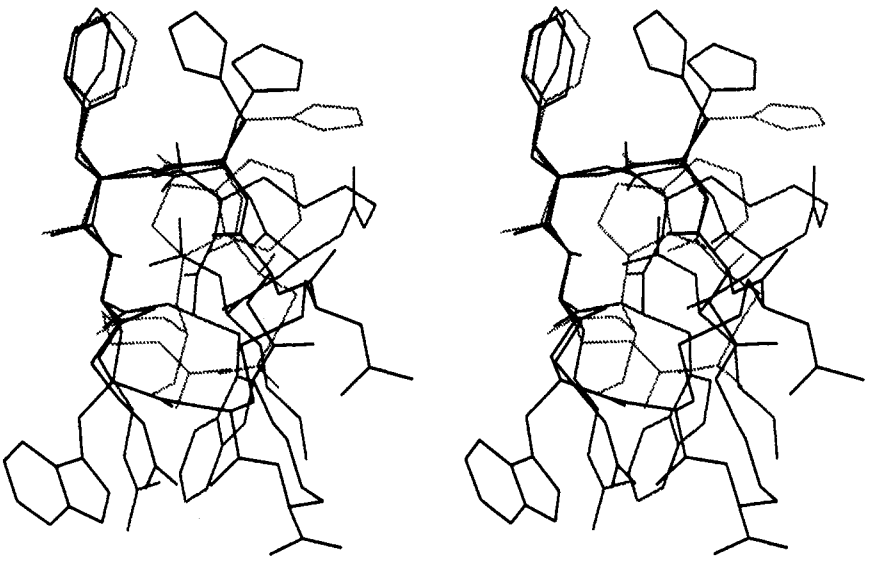

Figure 5. Superimposed stereoviews of the bicyclic analogue **VI** (conformer 4; bold lines), Ac-[Nle^4,Asp^5,DPhe^7,Lys^{10}]α-MSH(4–10)-NH_2 (bioactive conformation; semibold lines), and [DPhe^7]α-MSH (bioactive conformation; shadow lines). Superposition was performed by best fit matching of C^{α} and C^{β} atoms of the tripeptide His^6-DPhe^7-Arg^8. Residues 1–4 and 10–13 of [DPhe^7]α-MSH and all hydrogen atoms were omitted for clarity.

MSH and Ac-[Nle^4,Asp^5,DPhe^7,Lys^{10}]α-MSH(4–10)-NH_2 models, while the C^{α} and C^{β} atoms of Trp^9 in these three conformations do not overlap (Figure 5). Thus, the decreased biological potency of analogue **VI**, compared with potencies of α-MSH and the superpotent monocyclic lead compounds, may be explained by "incomplete" binding to the receptor by all the key side chain moieties of the His-DPhe-Arg-Trp sequence. None of the low-energy conformers of analogue **VII** matches the tripeptide 6–8 of the proposed bioactive conformation of [DPhe^7]α-MSH to within 0.50 Å. It can be noted that the models for the bioactive conformations proposed for Ac-[Cys^4,Cys^{10}]α-MSH(4–10)-NH_2 fit the tripeptide 6–8 of the bicyclic analogues better than the tripeptide 7–9, although in this case the matching is not very close (minimum rms deviations are about 0.8 Å, data not shown).

Conformer 4 of analogue **VI** fits equally well the proposed bioactive conformation for residues 6–8 in both the linear and cyclic superagonists [DPhe^7]α-MSH and Ac-[Nle^4,Asp^5,DPhe^7,Lys^{10}]α-MSH(4–10)-NH_2, respectively. In this context it should be noted that conformer 3 of analogue **VI** and conformer 4 of analogue **VII** closely match the C^{α} and C^{β} atoms of the tripeptide DPhe-Arg-Trp sequence for the bioactive conformation proposed[49] for the superagonist Ac-[Nle^4,Asp^5,DPhe^7,Lys^{10}]α-MSH(4–10)-NH_2. Consideration of the bioactivity of the tripeptides Ac-His^6-DPhe^7-Arg^8-NH_2 and Ac-DPhe^7-Arg^8-Trp^9-NH_2[57] in both bioassay systems allows us to further speculate on the relevant modeled conformations. The 6–8 tripeptide Ac-His^6-DPhe^7-Arg^8-NH_2 demonstrated no biological activity at concentrations up to 10^{-5} M, Table 1. The 7–9 tripeptide, however, maintained full agonistic activity in both the frog and lizard assays with EC_{50} values of 10 and 1.0 μM, respectively, Table 1. This would suggest that the Trp^9 residue is critical for biological activity and can be considered as a critical residue for a melanotropin pharmacophore. Addition of His^6 to the 7–9 sequence of the linear fragment increases the potency 100-fold and clearly maintains a potentiating effect. These observations allow us to suggest that modeled conformations of the bicyclic analogue 7–9 region that closely match the previously proposed models may be weighted more in regards to being biologically relevant (Table 7). Superimposed stereoviews of these three analogues are shown in Figure 6. This allows us to offer an alternative

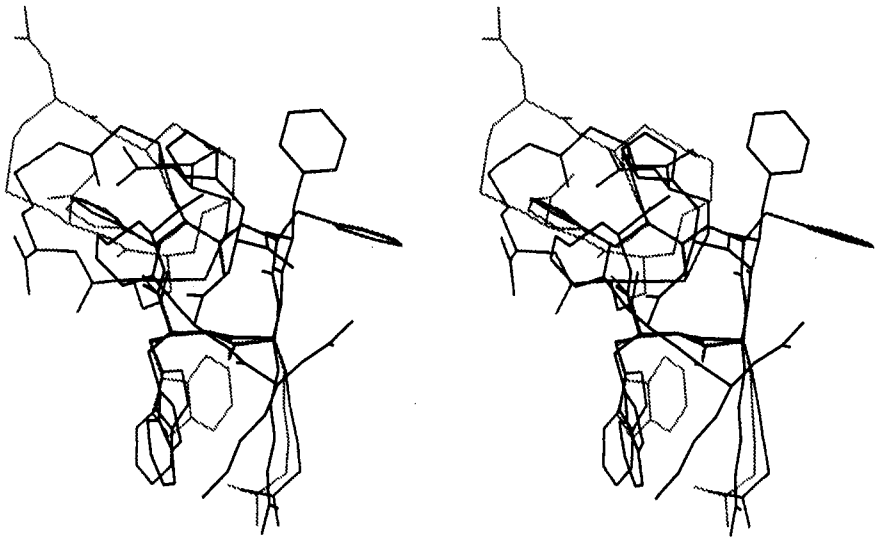

Figure 6. Superimposed stereoviews of Ac-[Nle^4,Asp^5,DPhe^7,Lys^{10}]α-MSH(4−10)-NH_2 (bioactive conformation; bold lines) and the bicyclic analogues **VI** (conformer 3; semibold lines) and **VII** (conformer 4; shadow lines). Superposition was performed by best fit matching of C^α and C^β atoms of the tripeptide DPhe^7-Arg^8-Trp^9. Hydrogen atoms were omitted for clarity.

model of "incomplete" binding to the receptor, wherein the bicyclic analogues bind to the receptor utilizing the side chains of residues 7−9, while the side chain of His^6 does not completely fit into its binding site. Conformer 3 of analogue **VI** and conformer 4 of analogue **VII**, which may be pertinent to this mode of binding, have very similar arrangement of the message side chain C^α and C^β atoms. This may help explain the equal potencies of analogues **VI** and **VII** in the lizard skin bioassay.

The bicyclic constraints that were made utilizing various side chain functionalities of α-MSH may alter χ space and ligand topology as well as the φ,ψ space of the peptide backbone. On the basis of the biological potencies, the topology of these bicyclic analogues that is being presented to the receptor is different from that of the superpotent monocyclic analogues. The constrained side chain moieties important for the melanotropin pharmacophores may be improperly sterically constrained by one of the two side chain cycles, and thus optimal presentation of the key residues His^6-DPhe^7-Arg^8-Trp^9 for receptor recognition may not be possible. While the monocyclic analogues contain one side chain to side chain cycle, this constraint apparently allows for the proper χ space (side chain χ^1 and χ^2 torsion angles) presentation of the pharmacophore residues, adding just the right amount of backbone constraint to adjust φ,ψ space, to present the predominant conformations for biological activity. Because of the close structural similarity of the bicyclic analogues, one can assume that this incomplete binding takes place in a conformation common to all the compounds examined in this study. Another possibility is that the dynamic properties required for superpotent biological activity cannot be obtained due to the increased conformational constraints induced by dual side chain cyclizations. Further examination of the effects of converting a linear analogue to disulfide and lactam monocyclic derivatives, and comparison with the bicyclic analogues presented in this study, may provide insight into the conformational or dynamic properties that these bicyclic analogues are unable to attain. Alternatively appropriate modifications of the bicyclic analogues may lead to antagonists.

Experimental Section

Materials. TLC was performed using Merck silica gel 60 F_{254} plates and the following solvent systems: (A) 1-butanol/acetic acid/pyridine/water (5:5:1:4), (B) ammonium hydroxide/water/2-propanol (1:1:3:), and (C) upper phase of 1-butanol/acetic acid/water (4:1:5). The peptides were detected on the TLC plates using iodine vapor. Final peptide purification was achieved by a semipreparative RP-HPLC C_{18} bonded silica column (Vydac 218TP1010, 1.0 × 25 cm). The peptides were eluted with a linear acetonitrile gradient (10−50%) over 40 min at a flow rate of 5.0 mL/min, with a constant concentration of TFA (0.1% v/v). The linear gradient was generated with a Perkin-Elmer 410 LC Bio pump system. The separations were monitored at 280 nm and integrated with a Perkin-Elmer LC-235 diode array detector. Amino acid analyses were performed at the University of Arizona Biotechnology Core Facility. The system used was an Applied Biosystems Model 420A amino acid analyzer with automatic hydrolysis (vapor phase at 160 °C for 1 h 40 min using 6 N HCl) and precolumn phenylthiocarbamyl-amino acid (PTC-AA) analysis. No corrections are made for amino acid decomposition. Optical rotation values were measured on a Fisher Autopol III at 589 nm in 10% acetic acid. The pMBHA resin (0.37 mmol of NH_2/g) was purchased from Peptides International Inc. (Louisville, KY 40224). N^α-Boc-protected amino acids and amino acid derivatives were purchased from Bachem (Torrance, CA) or prepared by standard methods. All amino acids were of the L-configuration except for phenylalanine which was of the D-configuration. The reactive side chains of the amino acids were protected as follows: Lys, with fluorenylmethyloxycarbonyl (Fmoc); Asp, with fluorenylmethyl ester (OFm); Glu, with fluorenylmethyl ester (OFm); His, with benzyloxymethyl (Bom); Arg, with tosyl (Tos); Trp, with formyl (For); Ser, with *O*-benzyl (O-Bzl); and Tyr, with 2,6-dichlorobenzyl (2-ClBzl). All reagents and solvents were ACS grade or better and used without further purification. The purity of the finished peptides was checked by TLC in three solvents and analytical RP-HPLC at 280 and 220 nm. In all cases they were greater than 91% pure as determined by these methods. The structures of the pure peptides were confirmed by fast atom bombardment (FAB) mass spectrometry and amino acid analysis (not corrected for amino acid destruction), Table 8.

Peptide Synthesis. The peptides were synthesized using a Vega 1000, 250 synthesizer or a manual synthesizer adapted from previously published methods.[39,55]

Ac-Ser-Tyr-Ser-Cys-Glu-His-DPhe-Arg-Trp-Cys-Lys-Pro-Val-NH_2 (I). A 4.4 g sample of pMBHA resin (0.37 mmol of NH_2/g of resin) was neutralized with 10% DIEA in DCM (2 ×

Table 8. Physicochemical Properties of the Bicyclic Analogues

peptide	optical rotation, $[\alpha]_{598}^{24}$ (in 10% aqueous HOAc) (deg)	R_f, TLC solvents[a] A	B	C	k' [b] HPLC	FAB-MS obsd M	calcd M
I	−53.75 (c = 0.80)	0.74	0.69	0.08	4.2	1663	1663
II	−84.00 (c = 0.67)	0.74	0.70	0.08	4.2	1326	1326
III	−40.59 (c = 1.13)	0.75	0.75	0.08	3.6	1130	1130
IV	−52.50 (c = 0.27)	0.75	0.70	0.06	4.7	1649	1649
V	−48.00 (c = 0.33)	0.77	0.81	0.06	4.3	1312	1312
VI	−42.86 (c = 0.47)	0.78	0.68	0.10	4.0	1116	1116
VII	−86.25 (c = 0.53)	0.75	0.67	0.06	3.5	1116	1116

[a] R_f values on thin-layer chromatograms of silica gel were observed in the following solvent systems: (A) 1-butanol/acetic acid/pyridine/water (5:5:1:4), (B) ammonium hydroxide/water/2-propanol (1:1:3), and (C) upper phase of 1-butanol/acetic acid/water (4:1:5). [b] HPLC k' = [(peptide retention time − solvent retention time)/solvent retention time] in a solvent system of 10% acetonitrile in 0.1% trifluoroacetic acid and a gradient to 50% acetonitrile over 40 min. An analytical Vydac C_{18} column was used with a flow rate of 1.5 mL/min.

50 mL) followed by a DCM wash (4 × 50 mL). The amino acid Nα-Boc-Val was coupled to the resin in DCM using DIC (6.5 mmol) and HOBT (6.5 mmol) as coupling reagents for 2 h. The Nα-Boc protecting group was removed by washing the resin for 2 min in 50% TFA, 2% anisole in DCM (1 × 50 mL) followed by a 20 min 50% TFA, 2% anisole in DCM wash (1 × 50 mL). The resin was then washed with DCM (3 × 50 mL), neutralized with 10% DIEA in DCM (2 × 50 mL), and washed with DCM (4 × 50 mL). The sequential addition of the amino acids Nα-Boc-Pro, Nα-Boc-Lys(Nε-Fmoc), Nα-Boc-Cys(pMB), Nα-Boc-Trp(Ni-For), Nα-Boc-Arg(Nγ-Tos), Nα-Boc-DPhe, and Nα-Boc-His(Nπ-Tos) utilized a 4-fold excess (6.5 mmol) and the same coupling and Nα-Boc removal conditions described above. At this stage, the Nα-Boc group on His was left in place, and the resin was washed with DCM (6 × 50 mL) and dried *in vacuo* to yield 6.74 g of Boc-His(Nπ-Tos)-DPhe-Arg(Nγ-Tos)-Trp-(Ni-For)-Cys(pMB)-Lys(Nε-Fmoc)-Pro-Val-resin.

From this precursor, 3.3 g (approximately 0.8 mmol) was taken, and a 1.5-fold excess (1.2 mmol) of the amino acid Nα-Boc-Glu(γ-OFm) was coupled in NMP to the growing peptide chain using BOP (1.4-fold excess) and DIEA (1.6-fold excess) as coupling reagents. The Fmoc and OFm protecting groups were removed by treatment with 20% piperidine in DMF (1 × 50 mL) for 20 min. The free acid side chain was coupled to the free amine side chain by the addition of BOP (5-fold excess) and DIEA (6-fold excess) in NMP for 2 h. This process was repeated three times until the ninhydrin tests were negative. The amino acid Nα-Boc-Cys(pMB) was then coupled in DCM using the previously described DIC and HOBT conditions. The resin was dried *in vacuo* to yield 3.0 g of Nα-Boc-Cys(pMB)-Glu-His(Nπ-Tos)-DPhe-Arg(Ng-Tos)-Trp(Ni-For)-Cys(pMB)-Lys-Pro-Val-resin.

To 1.5 g of this precursor was coupled 1.6 mmol of the amino acids Nα-Boc-Ser(O-Bzl), Nα-Boc-Tyr(2-ClZ), and Nα-Boc-Ser-(O-Bzl) in DCM, and the Nα-Boc protecting groups were removed. The N-terminal acetylation was carried out by the addition of 2 mL of acetic anhydride and 1 mL of pyridine, for 20 min. The resin was washed with DCM (6 × 50 mL) and dried *in vacuo* to yield 1.8 g. The dry resin was divided equally into two HF reaction vessels, and 0.5 g of *p*-thiocresol, 0.5 g of *p*-cresol, and 10 mL of anhydrous HF were added to each vessel. The mixture was stirred at 0 °C for 50 min. To remove the scavengers, anhydrous ethyl ether (5 × 30 mL) was added to each vessel and the contents were filtered using a course glass frit. The crude peptide was dissolved in glacial acetic acid (4 × 50 mL) and lyophilized to give 225 mg of crude peptide.

The peptide was then dissolved in 20 mL of water and 3 mL of methanol. An oxidizing solution consisting of 200 mL of 0.01 M potassium ferricyanide, 10 mL of saturated ammonium acetate, 20 mL of acetonitrile, and 10 mL of water was adjusted to pH = 8.5 with a few drops of concentrated ammonium hydroxide. The peptide solution was taken up in a 50 mL syringe and transferred to the oxidizing solution via a syringe pump at a rate of 1.5 mL/h. When the transfer was complete, the pH was adjusted to 4.5 with glacial acetic acid. Amberlite resin (IRA-68 HCl form) was added to the mixture and left to mix for 45 min. The Amberlite resin was filtered off, with the solution containing the peptide concentrated and lyophilized to give 7.6 g of salt and peptide. Then 2.6 g of the salt/peptide mixture was purified by preparative RP-HPLC to yield 22 mg of pure peptide. Amino acid analysis of **I** was as follows: Ser (1.79), Tyr (1.05), Glu (1.05), His (0.97), Phe (1.00), Arg (0.99), Cys (1.89), Lys (0.94), Pro (1.10), Val (1.05). The other analytical properties of the peptide are given in Table 8.

Ac-Cys-Glu-His-DPhe-Arg-Trp-Cys-Lys-Pro-Val-NH$_2$ (II). A 1.5 g of sample Nα-Boc-Cys(pMB)-Glu-His(Nπ-Tos)-DPhe-Arg-(Nγ-Tos)-Trp(Ni-For)-Cys(pMB)-Lys-Pro-Val-resin was Nα deprotected and N-terminal acetylated in DCM using 2 mL of acetic anhydride and 1 mL of pyridine for 21 min. After drying *in vacuo*, 1.30 g of resin, 0.7 g of *p*-cresol, 0.7 g of *p*-thiolcresol, and 13 mL of anhydrous HF were mixed at 0 °C for 50 min. The workup was the same as for compound **I** and a yield of 100 mg of crude product resulted. Then disulfide cyclization on a 50 mg sample was performed as described for compound **I** to yield 1.32 g of peptide/salt. From this, 750 mg was purified by RP-HPLC to yield 14 mg of pure peptide. Amino acid analysis of **II** was as follows: Glu (1.10), His (1.03), Phe (0.95), Arg (1.04), Cys (1.81), Lys (0.91), Pro (1.08), Val (1.10). The other analytical properties of **II** are given in Table 8.

Ac-Cys-Glu-His-DPhe-Arg-Trp-Cys-Lys-NH$_2$ (III). A 1.35 g sample of pMBHA resin (0.37 mmol of NH_2/g of resin) was treated with 10% DIEA in DCM (2 × 30 mL) and then washed with DCM (4 × 30 mL). Nα-Boc-Lys(Nε-Fmoc) in 2-fold excess (0.99 mmol) was coupled to the resin in NMP using BOP (1.09 mmol) and DIEA (1.19 mmol) as coupling reagents. The Nα-Boc protecting group was removed using 50% TFA, 2% anisole in DCM (2 min × 30 mL, 20 min × 30 mL). The resin was washed with DCM (3 × 30 mL) and treated with 10% DIEA in DCM (2 × 30 mL) followed by successive washing with DCM (4 × 30 mL). The amino acid residues Nα-Boc-Cys(pMB), Nα-Boc-Trp(Ni-For), Nα-Boc-Arg(Nγ-Tos), Nα-Boc-DPhe, and Nα-Boc-His(Nπ-Tos) in 4-fold excess (1.98 mmol) were coupled sequentially in DCM using DIC (2 mmol) and HOBT (2 mmol) as coupling reagents. The Nα-Boc protecting groups were removed as described above. Nα-Boc-Glu(γ-OFm) was coupled using the BOP coupling conditions described above. The Fmoc and OFm side chain protecting groups were removed by treatment with 20% piperidine in DMF for 20 min. The lactam cyclization was done using BOP (2.48 mmol) and DIEA (2.98 mmol) in NMP for 2 h as coupling conditions. The cyclization was complete after three couplings and tested ninhydrin negative. The coupling of Nα-Boc-Cys(pMB) using DIC/HOBT coupling conditions was followed by N-terminal acetylation using 2 mL of acetic anhydride and 1 mL of pyridine in DCM for 20 min. The resin was dried *in vacuo* and weighed to give 1.73 g of peptide resin which was split into two portions of 0.86 g each.

Then 0.4 g of *p*-thiocresol, 0.4 g of *p*-cresol, and 8 mL of anhydrous HF were added to each vessel and mixed for 50 min at 0 °C. The vessels were washed and filtered using anhydrous ethyl ether (5 × 30 mL). The peptide was dissolved in glacial acetic acid (4 × 50 mL) and lyophilized producing 420 mg of crude product.

Then 210 mg was cyclized by dissolving it in 10 mL of water, 9 mL of acetonitrile, and 6 mL of methanol. This was added via a syringe at a rate of 1.5 mL/h to an oxidizing solution containing 200 mL of 0.01 M potassium ferricyanide, 10 mL of saturated ammonium acetate, 20 mL of acetonitrile, and 10 mL of water and adjusted to pH = 8.5 with a few drops of concentrated ammonium hydroxide. When the transfer was complete, the pH was adjusted to 4.5 with glacial acetic acid. Amberlite resin (IRA-68 HCl form) was added to the solution which was mixed for 45 min. The Amberlite resin was filtered

off; the solution containing the peptide was concentrated and lyophilized to give 8.3 g of salt and peptide. Then 3.4 g of the salt/peptide mixture underwent preparative RP-HPLC to yield 25 mg of pure peptide. Amino acid analysis of **III** was as follows: Glu (1.03), His (1.02), Phe (1.00), Arg (1.02), Cys (1.80), Lys (0.90). The other analytical properties for the final product are given in Table 8.

Ac-Ser-Tyr-Ser-Cys-Asp-His-DPhe-Arg-Trp-Cys-Lys-Pro-Val-NH_2 (IV). A 3.3 g sample of N^{α}-Boc-His(N^{π}-Tos)-DPhe-Arg(N^{γ}-Tos)-Trp(N^{i}-For)-Cys(pMB)-Lys(N^{ϵ}-Fmoc)-Pro-Val-resin was N^{α}-Boc deprotected using 50% TFA, 2% anisole in DCM (2 min × 30 mL, 20 min × 30 mL). The resin was washed with DCM (3 × 30 mL) and treated with 10% DIEA in DCM (2 × 30 mL) followed by successive washing with DCM (4 × 30 mL). The N^{α}-Boc-Asp(β-OFm) was then coupled in NMP to the growing peptide chain using BOP (1.12 mmol) and DIEA (1.28 mmol) as coupling reagents. The N^{α}-Boc groups were removed as previously described, and the Fmoc and OFm side chain protecting groups were removed by treatment with 20% piperidine in DMF for 20 min. The lactam bridge cyclization utilized BOP (4.0 mmol) and DIEA (4.8 mmol) in NMP for 2 h as coupling conditions. The cyclization was completed after three couplings and tested ninhydrin negative. The amino acid N^{α}-Boc-Cys(pMB) was coupled in DCM using the previously described DIC and HOBT conditions. The resin was dried *in vacuo* to yield 3.16 g of N^{α}-Boc-Cys(pMB)-Asp-His(N^{π}-Tos)-DPhe-Arg(N^{γ}-Tos)-Trp(N^{i}-For)-Cys(pMB)-Lys-Pro-Val-resin.

To a 1.5 g portion of this precursor was coupled 1.6 mmol of the amino acids N^{α}-Boc-Ser(O-Bzl), N^{α}-Boc-Tyr(2,4-Cl_2Bzl), and N^{α}-Boc-Ser(O-Bzl) in DCM, and the N^{α}-Boc protecting groups were removed. N-terminal acetylation was accomplished by addition of 2 mL of acetic anhydride and 1 mL of pyridine which were mixed for 20 min. Then the resin was washed with DCM (6 × 50 mL) and dried *in vacuo* to yield 1.8 g. The dry resin was divided equally into two HF reaction vessels followed by the addition of 0.5 g of *p*-thiocresol, 0.5 g of *p*-cresol, and 10 mL of anhydrous HF to each vessel. The mixture was stirred at 0 °C for 50 min. To remove the scavengers, anhydrous ethyl ether (5 × 30 mL) was added to each vessel and filtered using a course glass frit. The crude peptide was dissolved in glacial acetic acid (4 × 50 mL) and lyophilized to give 200 mg of crude peptide.

A 100 mg portion of peptide was dissolved in 30 mL of water and 5 mL of acetonitrile. An oxidizing solution consisting of 200 mL of 0.01 M potassium ferricyanide, 10 mL of saturated ammonium acetate, 20 mL of acetonitrile, and 10 mL of water was adjusted to pH = 8.5 with a few drops of concentrated ammonium hydroxide. The peptide solution was taken up in a 50 mL syringe and transferred to the oxidizing solution via a syringe pump at a rate of 1.5 mL/h. When the transfer was complete, the pH was adjusted to 4.5 with glacial acetic acid. Amberlite resin (IRA-68 HCl form) was added to the mixture and left to stir for 45 min. The Amberlite resin was filtered off, and the solution containing the peptide was concentrated to give 6.7 g of salt and peptide. A 1.5 g portion of the salt/peptide mixture was purified by RP-HPLC to yield 14 mg of pure peptide. Amino acid analysis of **IV** was as follows: Ser (2.17), Tyr (0.90), Asp (0.94), His (0.90), Phe (1.00), Arg (0.95), Cys (1.84), Lys (0.91), Pro (1.12), Val (1.01). The other analytical properties of the peptide product are given in Table 8.

Ac-Cys-Asp-His-DPhe-Arg-Trp-Cys-Lys-Pro-Val-NH_2 (V). A 1.5 g sample of N^{α}-Boc-Cys(pMB)-Asp-His(N^{π}-Tos)-DPhe-Arg(N^{γ}-Tos)-Trp(N^{i}-For)-Cys(pMB)-Lys-Pro-Val-resin was N^{α}-Boc deprotected using 50% TFA, 2% anisole in DCM (2 min × 30 mL, 20 min × 30 mL). The peptide resin was washed with DCM (3 × 30 mL) and treated with 10% DIEA in DCM (2 × 30 mL) followed by successive washing with DCM (4 × 30 mL). The N-terminal was acetylated and the resin washed with DCM (6 × 30 mL) and dried *in vacuo* to yield 1.18 g of peptide-resin.

This was split into two portions, and 0.6 g of *p*-thiocresol, 0.6 g of *p*-cresol, and 12 mL of anhydrous HF were added to each vessel. The mixture was stirred at 0 °C for 50 min and the HF removed in high vacuum. To remove the scavengers, anhydrous ethyl ether (5 × 30 mL) was added to each vessel and filtered using a course glass frit. The crude peptide was dissolved in glacial acetic acid (4 × 50 mL) and lyophilized to give 60 mg of crude peptide.

Then 30 mg was dissolved in 20 mL of water, 2 mL of methanol, and 2 mL of acetonitrile. The peptide solution was taken up in a 50 mL syringe and transferred to the oxidizing solution (consisting of 200 mL of 0.01 M potassium ferricyanide, 10 mL of saturated ammonium acetate, 20 mL of acetonitrile, and 10 mL of water, adjusted to pH = 8.5 with a few drops of concentrated ammonium hydroxide) via a syringe pump at a rate of 1.5 mL/h. When the transfer was complete, the pH was adjusted to 4.5 with glacial acetic acid. Amberlite resin (IRA-68 HCl form) was added to the solution and left to mix for 45 min. The Amberlite resin was filtered off, and the solution containing the peptide was concentrated to give 6.8 g of salt and peptide. A 1.2 g sample of the salt/peptide mixture was purified by preparative RP-HPLC to yield 11 mg of pure peptide. Amino acid analysis of **V** was as follows: Asp (0.99), His (1.03), Phe (0.97), Arg (1.03), Cys (1.92), Lys (0.87), Pro (1.10), Val (1.07). The other analytical properties of the final product are given in Table 8.

Ac-Cys-Asp-His-DPhe-Arg-Trp-Cys-Lys-NH_2 (VI). A 1.68 g sample of pMBHA resin (0.37 mmol of NH_2/g of resin) was treated with 10% DIEA in DCM (2 × 30 mL) and then washed with DCM (4 × 30 mL). N^{α}-Boc-Lys(N^{ϵ}-Fmoc) in 2-fold excess (1.24 mmol) was coupled to the resin in NMP using BOP (1.49 mmol) and DIEA (1.63 mmol) as coupling reagents. The N^{α}-Boc protecting group was removed using 50% TFA, 2% anisole in DCM (2 min × 30 mL, 20 min × 30 mL). The resin was washed with DCM (3 × 30 mL) and treated with 10% DIEA in DCM (2 × 30 mL) followed by successive washing with DCM (4 × 30 mL). The amino acids N^{α}-Boc-Cys(pMB), N^{α}-Boc-Trp(N^{i}-For), N^{α}-Boc-Arg(N^{γ}-Tos), N^{α}-Boc-DPhe, and N^{α}-Boc-His(N^{π}-Tos) in 4-fold excess (2.48 mmol) were coupled sequentially to the peptide-resin in DCM using DIC (2.5 mmol) and HOBT (2.5 mmol) as coupling reagents. The N^{α}-Boc protecting groups were removed as described above. The peptide resin was washed with DCM (6 × 30 mL) and dried *in vacuo*. One-half was taken, and N^{α}-Boc-Asp(β-OFm) was coupled using the BOP coupling conditions described above for **I**. The Fmoc and OFm side chain protecting groups were removed by treatment with 20% piperidine in DMF for 20 min. The lactam bridge was formed using BOP (3.4 mmol) and DIEA (4.1 mmol) in NMP for 2 h as coupling conditions. The cyclization was complete after two couplings, as determined by the ninhydrin test. The N^{α}-Boc-Cys(pMB) was coupled to the peptide-resin using DIC/HOBT followed with N-terminal acetylation with 2 mL of acetic anhydride and 1 mL of pyridine in DCM for 20 min. The protected peptide resin was dried *in vacuo* and weighed 1.3 g.

A mixture of 1.2 g of resin, 0.6 g of *p*-thiocresol, 0.6 g of *p*-cresol, and 12 mL of anhydrous HF was stirred and mixed for 50 min at 0 °C. The HF and cresols were removed *in vacuo*, and the resin/peptide/byproduct was washed and filtered using anhydrous ethyl ether (5 × 30 mL). The peptide was dissolved in glacial acetic acid (4 × 50 mL) and lyophilized producing 890 mg of crude peptide.

Then 320 mg of the peptide was dissolved in methanol and diluted to 1 L with degassed water. The pH was adjusted to 10.3 with a few drops of concentrated ammonium hydroxide, 31 mL of freshly prepared 0.01 M potassium ferricyanide was added to the solution, and the solution was mixed for 30 min. The pH was adjusted to 4.5 with glacial acetic acid. Amberlite resin (IRA-68 HCl form) was added to the mixture and left to mix for 45 min. The Amberlite resin was filtered off, and the solution containing the bicyclized peptide was concentrated and lyophilized to give 14.4 g of salt and peptide. Then 2.98

g of the salt/peptide mixture was purified by preparative RP-HPLC to yield 13 mg of pure peptide. Amino acid analysis of **VI** was as follows: Asp (0.99), His (0.98), Phe (1.00), Arg (1.00), Cys (1.82), Lys (0.92). The other analytical properties of the peptide are given in Table 8.

Ac-Cys-Asp-His-DPhe-Arg-Trp-Lys-Cys-NH_2 (VII). A 4.58 g sample of pMBHA resin (0.37 mmol of NH_2/g of resin) was washed with 10% DIEA in DCM (2 × 30 mL) and then with DCM (4 × 30 mL). A 4-fold excess of N^{α}-Boc-Cys(pMB) was coupled to the resin in DCM using DIC (6.8 mmol) and HOBT (6.8 mmol) as coupling reagents. The N^{α}-Boc protecting group was removed using 50% TFA, 2% anisole in DCM (2 min × 50 mL, 20 min × 50 mL). The resin was washed with DCM (3 × 50 mL) and treated with 10% DIEA in DCM (2 × 50 mL) followed by successive washing with DCM (4 × 50 mL). N^{α}-Boc-Lys(N^{ϵ}-Fmoc) in 1.2-fold excess (1.24 mmol) was coupled to the resin in NMP using BOP (2.38 mmol) and DIEA (2.7 mmol) as coupling reagents and followed by N^{α}-Boc deprotection. The amino acids N^{α}-Boc-Trp(N^{i}-For), N^{α}-Boc-Arg(N^{γ}-Tos), N^{α}-Boc-DPhe, and N^{α}-Boc-His(N^{π}-Tos) in 4-fold excess (6.8 mmol) were coupled sequentially in DCM using DIC (6.8 mmol) and HOBT (6.8 mmol) as coupling reagents. The N^{α}-Boc groups were removed as before (except for N^{α}-Boc-His(N^{π}-Tos)) and the N^{α}-Boc-protected peptide resin dried *in vacuo* to give 7.85 g.

Then 2.7 g of protected peptide resin was N^{α}-Boc deprotected, and N^{α}-Boc-Asp(β-OFm) was coupled using BOP (1.32 mmol) and DIEA (1.4 mmol) as coupling reagents. The Fmoc and OFm side chain protecting groups were removed by treatment with 20% piperidine in DMF for 20 min. The lactam bridge cyclization was accomplished using BOP (3.0 mmol) and DIEA (3.6 mmol) in NMP for 2 h. The cyclization was complete after three couplings and tested ninhydrin negative. N^{α}-Boc-Cys(pMB) was coupled and the N-terminal acetylated using 2 mL of acetic anhydride, 1 mL of pyridine in DCM for 20 min. The resin was washed with DCM (6 × 40 mL) and dried *in vacuo* to yield 2.15 g.

The resin was divided in two portions, and 0.6 g of *p*-thiocresol, 0.6 g of *p*-cresol, and 12 mL of anhydrous HF were added to each vessel. The mixture was stirred at 0 °C for 50 min, and the HF and cresols were removed *in vacuo*. To remove the scavengers, anhydrous ethyl ether (5 × 30 mL) was added to each vessel and filtered using a course glass frit. The crude peptide was dissolved in glacial acetic acid (4 × 50 mL) and lyophilized to give 60 mg of crude peptide.

Then 30 mg was dissolved in 20 mL of water, 3 mL of methanol, and 2 mL of acetonitrile. An oxidizing solution consisting of 200 mL of 0.01 M potassium ferricyanide, 10 mL of saturated ammonium acetate, and 30 mL of water was adjusted to pH = 8.5 with a few drops of concentrated ammonium hydroxide, and the peptide solution was taken up in a 50 mL syringe and transferred to the oxidizing solution via a syringe pump at a rate of 1.5 mL/h. When the transfer was complete, the pH was adjusted to 4.5 with glacial acetic acid. Amberlite resin (IRA-68 HCl form) was added to the mixture and left to mix for 45 min. The Amberlite resin was filtered off, and the solution containing the peptide was concentrated resulting in 1.98 g of salt and peptide. Then 1.2 g of the salt/peptide mixture was purified to yield 15 mg of pure peptide. Amino acid analysis of **VII** was as follows: Asp (1.02), His (1.06), Phe (1.00), Arg (1.12), Lys (0.92), Cys (1.80). The other analytical properties of **VII** are given in Table 8.

Energy Calculations. The energy calculations were performed using the ECEPP/2 force field[59,60] with associated rigid-valence geometry and all-trans amide bonds, including the amide bonds formed between the side chains of Asp/Glu and Lys. Electrostatic interactions were calculated with dielectric constant $\epsilon = 2.0$ using standard ECEPP atomic charges,[60] all side chains and terminal groups being considered electroneutral. In order to achieve most careful representation of local interactions in the backbone and in the vicinity of the disulfide and lactam bridges, α-hydrogens and methylene hydrogens in Cys, Asp, Glu, and Lys side chains were considered as separate atoms. Aliphatic and aromatic CH_n groups in the side chains of His, Phe, Arg, and Trp residues, as well as terminal methyl groups, were considered as united atoms with UNICEPP parameters for nonbonded interactions.[62]

Energy minimization was performed over all backbone and side chain torsion angles, including backbone ω angles inside the cycles, using a quasi-Newton algorithm, SUMSL.[48,49] In order to achieve ring closure with standard valence geometry in a bride moiety, target functions of minimization included harmonic penalty potentials:

$$U_{pen} = U_o(d - d_o)^2$$

where U_o is a force constant and d and d_o are current and target values of an interatomic distance. In intermediate buildup stages of cycle formation, one-side penalty potentials assuming $U_o = 0$ when $d < d_o$ were included into a target function of minimization in order to constrain selected interatomic distances to predetermined upper limit values. After minimization, residuals of penalty potentials were always subtracted from resulting values of target functions, in order to compare pure conformational energies.

Four penalty potentials recommended by Momany et al.[60] were employed to maintain the standard geometry of disulfide bridges with $C^{\beta}-S-S-C^{\beta}$ dihedral angles about ±90°. The lactam bridges between Asp/Glu and Lys side chains were closed in two consecutive steps of minimization employing two sets of penalty potentials. In the first preliminary step, the $C^{\delta}-C^{\epsilon}$ bond of lysine was removed and the $N^{\zeta}H-C^{\epsilon}$ group was included into an artificial Asp-CO-NHC$^{\alpha}$ or Glu-CO-NHC$^{\alpha}$ residue. Three penalty potentials with force constants of 100 kcal/mol Å^2 were applied to maintain $C^{\delta}-C^{\epsilon}$, $C^{\gamma}-C^{\epsilon}$, and $C^{\delta}-N^{\zeta}$ distances near the values corresponding to the standard $C^{\delta}-C^{\epsilon}$ bond length of 1.53 Å with adjacent bond angles of 110°. In the second step, C^{ϵ} and N^{ζ} atoms were attached to the lysine side chain, while their duplicates in Asp-CO-NHC$^{\alpha}$ and Glu-CO-NHC$^{\alpha}$ side chains were considered as noninteracting dummy atoms. Exact lactam cycle closure was attained with the aid of two penalty potentials (U_o = 100 kcal/mol Å^2, d_o = 0) which forced superposition of the real C^{ϵ} and N^{ζ} atoms with their dummy counterparts.

Comparison and Clustering of Conformations. The geometric similarity between a pair of conformers was checked by assessment of the best fit matching of the selected atomic centers.[63] In this study C^{α} and C^{β} atoms of residues 6–9 and C^{α} atoms of residues 5 and 7 were selected for the matching. rms deviation of the matching was taken as the measure of similarity (distance) between a pair of conformers, the conformers with rms ≤ 1.0 Å being regarded as similar. Matrices of square distances $(\text{rms})^2$ were calculated for the sets of low-energy conformers of each analogue under the study. A set of m conformers was partitioned into n clusters ($2 \le n < m/2$) using the criterion of minimum sum of square distances.[64] The partitioning was assumed satisfactory when the maximum rms within each cluster (diameter of a cluster) became less than 1.0 Å. Lowest energy conformers of each cluster were selected to represent a given compound for comparison with different analogues.

Frog and Lizard Skin Bioassays. The frog (*Rana pipiens*)[65] and lizard (*Anolis carolinensis*)[66,67] skin bioassays were utilized to determine the relative potencies of the synthetic melanotropins.[68] The assays measure the amount of light reflected from the surface of the skins *in vitro*. In response to melanotropic peptides, melanosomes within integumental melanocytes migrate from a perinuclear position into the dendritic processes of the pigment cells. This centrifugal organellar dispersion results in a change in color (darkening) of the skins which is measured by a Photovolt reflectometer and is expressed as the percent response compared to the initial (time zero) reflectance value. Subsequent removal of a melanotropin such as α-MSH usually results in a rapid perinuclear (centripetal) reaggregation of melanosomes within melanocytes leading to a lightening of the skin back to their original (base) value.

Acknowledgment. This work was supported by a grant from the U.S. Public Health Service (DK17420).

References

(1) Lowry, P. J.; Scott, A. P. The Evolution of Vertebrate Corticotropin and Melanocyte Stimulating Hormone. *Gen. Comp. Endocrinol.* **1975**, *26*, 16–23.

(2) Hadley, M. E. *Endocrinology*, 3rd ed.; Prentice Hall: Englewood Cliffs, NJ, 1992; pp 179–207.

(3) Fenger, M. Proopiomelanocortin: α-Amidated and Related Peptides. *Scand. J. Clin. Lab. Invest.* **1990**, *50*, 229–245.

(4) Krieger, D. The Multiple Faces of Pro-Opiomelanocortin, A Prototype Precursor Molecule. *Clin. Res.* **1983**, *31*, 342–353.

(5) Pintar, J. E.; Schachtter, B.; Herman, A. B.; Durgerian, S.; Krieger, D. T. Characterization and Localization of Proopiomelanocortin Messenger RNA in the Adult Rat Testis. *Science* **1984**, *225*, 632–634.

(6) Saito, E.; Iwasa, S.; Odell, W. D. Widespread Presence of Large Molecular Weight Adrenocorticotropin-Like Substances in Normal Rat Extrapituitary Tissues. *Endocrinology* **1983**, *113*, 1010–1019.

(7) Tatro, J. B.; Reichlin, S. Specific Receptors for α-Melanocyte-Stimulating Hormone are Widely Distributed in Tissues of Rodents. *Endocrinology* **1987**, *121*, 1900–1907.

(8) Tatro, J. B. Melanotropin Receptors in the Brain are Differentially Distributed and Recognize Both Corticotropin and α-Melanocyte Stimulating Hormone. *Brain Res.* **1990**, *536*, 124–132.

(9) Lerner, A. B.; McGuire, J. S. Effect of Alpha- and Beta-Melanocyte Stimulating Hormones on the Skin Colour of Man. *Nature* **1961**, *189*, 176–179.

(10) Lerner, A. B.; McGuire, J. S. Melanocyte-Stimulating Hormone and Adrenocorticotrophic Hormone. Their Relation to Pigmentation. *New Engl. J. Med.* **1964**, *270*, 539–546.

(11) De Wied, D.; Jolles, J. Neuropeptides Derived from Pro-Opiocortin: Behavioral, Physiological, and Neurochemical Effects. *Physiol. Rev.* **1982**, *62*, 976–1059.

(12) De Wied, D.; Croiset, G. Stress Modulation of Learning and Memory Processes. *Methods Achieve Exp. Pathol.* **1991**, *15*, 167–199.

(13) Walker, J. M.; Akil, H.; Watson, S. J. Evidence for Homologous Actions of Pro-opiomelanocortin Products. *Science* **1980**, *210*, 1247–1249.

(14) Murphy, M. T.; Richards, D. B.; Lipton, J. M. Antipyretic Potency of Centrally Administered α-MSH. *Science* **1983**, *221*, 192–193.

(15) Villar, M.; Perassi, N.; Celis, M. E. Central and Peripheral Actions of α-MSH in the Thermoregulation of Rats. *Peptides* **1991**, *12*, 1441–1443.

(16) Rothwell, N. J.; Hardwick, A.; LeFeuvre, R. A.; Crosby, S. R.; White, A. Central Action of CRF on Thermogenesis are Mediated by Pro-opiomelanocortin Products. *Brain Res.* **1991**, *541*, 89–92.

(17) Krieger, D. T. Placenta as a Source of 'Brain' and 'Pituitary' Hormones. *Biol. Reprod.* **1982**, *26*, 55–71.

(18) Wilson, J. F. Levels of α-Melanotropin in the Human Fetal Pituitary Gland Throughout Gestation, in Adult Pituitary Gland and in Human Placenta. *Clin. Endocrinol.* **1982**, *17*, 233–242.

(19) Clark, D.; Thody, A. J.; Shuster, S.; Bowers, H. Immunoreactive α-MSH in Human Plasma in Pregnancy. *Nature* **1978**, *273*, 163–164.

(20) Silman, R. E.; Chard, T.; Lowry, P. J.; Smith, I.; Young, I. M. Human Fetal Pituitary Peptides and Parturition. *Nature* **1976**, *260*, 716–718.

(21) Challis, J. R. G.; Torosis, J. D. Is α-MSH a Trophic Hormone to Adrenal Function in the Fetus? *Nature* **1977**, *269*, 818–819.

(22) Hiltz, M. E.; Catania, A.; Lipton, J. M. Anti-Inflammatory Activity of α-MSH (11–13) Analogs: Influences of Alteration in Stereochemistry. *Peptides* **1991**, *12*, 767–771.

(23) Hiltz, M. E.; Lipton, J. M. Anti-Inflammatory Activity of COOH-Terminal Fragment of the Neuropeptide α-MSH. *FASEB J.* **1989**, *3*, 2282–2284.

(24) Cannon, J. G.; Tatro, J. B.; Reichlin, S.; Dinarello, C. A. α-MSH Inhibits Immunostimulatory and Inflammatory Action of Interleukin 1. *J. Immunol.* **1986**, *137*, 2232–2236.

(25) Mountjoy, K. G.; Robbins, L. S.; Mortrud, M. T.; Cone, R. D. The Cloning of a Family of Genes that Encode the Melanocortin Receptors. *Science* **1992**, *257*, 1248–1251.

(26) Chhajlani, V.; Wikberg, J. E. S. Molecular Cloning and Expression of the Human Melanocyte Stimulating Hormone Receptor cDNA. *FEBS Lett.* **1992**, *309*, 417–420.

(27) Chhajlani, V.; Muceniece, R.; Wikberg, J. E. S. Molecular Cloning of a Novel Human Melanocortin Receptor. *Biochem. Biophys. Res. Commun.* **1993**, *195*, 866–873.

(28) Gantz, I.; Konda, Y.; Tashiro, T.; Shimoto, Y.; Miwa, H.; Munzert, G.; Watson, S. J.; DelValle, J.; Yamada, T. Molecular Cloning of a Novel Melanocortin Receptor. *J. Biol. Chem.* **1993**, *268*, 8246–8250.

(29) Gantz, I.; Miwa, H.; Konda, Y.; Shimoto, Y.; Tashiro, T.; Watson, S. J.; DelValle, J.; Yamada, T. Molecular Cloning, Expression, and Gene Localization of a Fourth Melanocortin Receptor. *J. Biol. Chem.* **1993**, *268*, 15174–15179.

(30) Gantz, I.; Shimoto, Y.; Konda, Y.; Miwa, H.; Dickinson, C. J.; Yamada, T. Molecular Cloning, Expression, and Characterization of a Fifth Melanocortin Receptor. *Biochem. Biophys. Res. Commun.* **1994**, *200*, 1214–1220.

(31) Roselli-Rehfuss, L.; Mountjoy, K. G.; Robbins, L. S.; Mortrud, M. T.; Low, M. J.; Tatro, J. B.; Entwistle, M. L.; Simerly, R. B.; Cone, R. D. Identification of a Receptor for γ Melanotropin and Other Proopiomelanocortin Peptides in the Hypothalamus and Limbic System. *Proc. Natl. Acad. Sci. U.S.A.* **1993**, *90*, 8856–8860.

(32) Labbé, O.; Desarnaud, F.; Eggerickx, D.; Vassart, G.; Parmentier, M. Molecular Cloning of a Mouse Melanocortin 5 Receptor Gene Widely Expressed in Peripheral Tissues. *Biochemistry* **1994**, *33*, 4543–4549.

(33) Hruby, V. J. Conformational Restrictions of Biologically-Active Peptides Via Amino Acid Side-Chain Groups. *Life Sci.* **1982**, *31*, 189–199.

(34) Hruby, V. J.; Al-Obeidi, F.; Kazmierski, W. Emerging Approaches In The Molecular Design of Receptor-Selective Peptide Ligands - Conformational, Topographical And Dynamic Considerations. *Biochem. J.* **1990**, *268*, 249–262.

(35) Sawyer, T. K.; Hruby, V. J.; Darman, P. S.; Hadley, M. E. [half-Cys^4,half-Cys^{10}]-α-Melanocyte-Stimulating Hormone: A Cyclic α-Melanotropin Exhibiting Superagonist Biological Activity. *Proc. Natl. Acad. Sci. U.S.A.* **1982**, *79*, 1751–1755.

(36) Cody, W. L.; Mahoney, M.; Knittel, J. J.; Hruby, V. J.; de L. Castrucci, A. M.; Hadley, M. E. Cyclic Melanotropins. 9. 7-D-Phenylalanine Analogues of the Active-Site Sequence. *J. Med. Chem.* **1985**, *28*, 583–588.

(37) Sugg, E. E.; de L. Castrucci, A. M.; Hadley, M. E.; van Binst, G.; Hruby, V. J. Cyclic Lactam Analogues of Ac-[Nle^4]α-MSH$_{4-11}$-NH$_2$. *Biochemistry* **1988**, *27*, 8181–8188.

(38) Al-Obeidi, F.; Hadley, M. E.; Pettitt, B. M.; Hruby, V. J. Design of a New Class of Superpotent Cyclic α-Melanotropins Based on Quenched Dynamic Simulations. *J. Am. Chem. Soc.* **1989**, *111*, 3413–3416.

(39) Al-Obeidi, F.; Castrucci, A. M.; Hadley, M. E.; Hruby, V. J. Potent and Prolonged Acting Cyclic Lactam Analogues of α-Melanotropin: Design Based on Molecular Dynamics. *J. Med. Chem.* **1989**, *32*, 2555–2561.

(40) For a preliminary report, see: Nikiforovich, G. V.; Sharma, S. D.; Hadley, M. E.; Hruby, V. J. Design of Different Conformational Isomers of the Same Peptide: α-Melanotropin In *Peptides: Chemistry and Biology*; Smith, J. A., Rivier, J. E., Eds.; ESCOM: Leiden, 1992; pp 389–392. Details will be published elsewhere.

(41) Bódi, J.; Medzihradszky-Schweiger, H.; Süli-Vargha, H. Synthesis and Biological Activity of Cyclic Melanotropin Peptides. In *Peptides*; G.E., Andreu, D., Eds.; ESCOM Science: Leiden, 1991; pp 690–691.

(42) Nikiforovich, G. V.; Rozenbilt, S. A.; Shenderovich, M. D.; Chipens, G. I. Possible Bioactive Conformation of α-Melanotropin. *FEBS Lett.* **1984**, *170*, 315–320.

(43) Hill, P. S.; Smith, D. D.; Slaninova, J.; Hruby, V. J. Bicyclization of a Weak Oxytocin Agonist Produces a Highly Potent Oxytocin Antagonist. *J. Am. Chem. Soc.* **1990**, *112*, 3110–3113.

(44) Veber, D. F.; Freidinger, R. M.; Perlow, D. S.; Paleveda, W. J.; Holly, F. W.; Strachan, R. G.; Nutt, R. F.; Arison, B. H.; Homnick, C.; Randall, W. C.; Glitzer, M. S.; Saperstein, R.; Hirschmann, R. A Potent Cyclic Hexapeptide Analogue of Somatostatin. *Nature* **1981**, *292*, 55–58.

(45) Nutt, R. F.; Veber, D. F.; Saperstein, R. Synthesis of Nonreducible Bicyclic Analogues of Somatostatin. *J. Am. Chem. Soc.* **1980**, *102*, 6539–6545.

(46) Hruby, V. J.; Al-Obeidi, F.; Sanderson, D. G.; Smith, D. D. Synthesis of Cyclic Peptides by Solid Phase Methods. In *Innovations and Perspectives in Solid Phase Synthesis*; Epton, R., Ed.; SPCC (U.K.) Ltd.: Oxford, England, 1989; pp 197–203.

(47) Kaiser, E.; Colescott, R. L.; Bossinger, C. D.; Cook, P. I. Color Test for Detection of Free Terminal Amino Groups in the Solid-Phase Synthesis of Peptides. *Anal. Biochem.* **1970**, *34*, 595–598.

(48) For a preliminary report, see: Sharma, S. D.; Nikiforovich, G. V.; Jiang, J.; Castrucci, A. M.; Hadley, M. E.; Hruby, V. J. A New Class of Positively Charged Melanotropin Analogs: A New Concept in Peptide Design. In *Peptides 1992*; Schneider, C. H., Eberle, A. N., Eds.; ESCOM: Leiden, 1993; pp 95–96.

(49) For a preliminary report, see: Sharma, S. D.; Nikiforovich, G. V.; Jiang, J.; Castrucci, A. M.; Hadley, M. E.; Hruby, V. J. Cationized Melanotropin Analogues: Structure-Function Relationships. In *Peptides: Chemistry and Biology*; Hodges, R. A., Smith, J. A., Eds.; ESCOM: Leiden, 1994; pp 398–399.

(50) Nikiforovich, G. V.; Hruby, V. J.; Prakash, O.; Gehrig, C. A. Topographical Requirements for δ-Selective Opioid Peptides. *Biopolymers* **1991**, *31*, 941–955.

(51) Zimmerman, S. S.; Scheraga, H. A. Influence the Local Interactions on Protein Structure. I. Conformational Energy Studies of N-Acetyl-N'-methylamides of Pro-X and X-Pro. *Biopolymers* **1977**, *16*, 811–843.
(52) Hruby, V. J.; Wilkes, B. C.; Hadley, M. E.; Al-Obeidi, F.; Sawyer, T. K.; Staples, D. J.; DeVaux, A.; Dym, O.; Castrucci, A. M.; Hintz, M. F.; Riehm, J. P.; Rao, K. R. α-Melanotropin: The Minimal Active Sequence in the Frog Skin Bioassay. *J. Med. Chem.* **1987**, *30*, 2126–2130.
(53) Castrucci, A. M. L.; Hadley, M. E.; Sawyer, T. K.; Wilkes, B. C.; Al-Obeidi, F.; Staples, D. J.; DeVaux, A. E.; Dym, O.; Hintz, M. F.; Riehm, J.; Rao, K. R.; Hruby, V. J. α-Melanotropin: The Minimal Active Sequence in the Lizard Skin Bioassay. *Gen. Comp. Endocrinol.* **1989**, *73*, 157–163.
(54) Sawyer, T. K.; Staples, D. J.; de L. Castrucci, A. M.; Hadley, M. E.; Al-Obeidi, F. A.; Cody, W. L.; Hruby, V. J. α-Melanocyte Stimulating Hormone Message and Inhibitory Sequences: Comparative Structure-Activity Studies on Melanocytes. *Peptides* **1990**, *11*, 351–357.
(55) Cody, W. L.; Wilkes, B. C.; Muska, B. J.; Hruby, V. J.; de L. Castrucci, A. M.; Hadley, M. E. Cyclic Melanotropins. 5. Importance of the C-Terminal Tripeptide (Lys-Pro-Val). *J. Med. Chem.* **1984**, *27*, 1186–1190.
(56) Hruby, V. J.; Wilkes, B. C.; Cody, W. L.; Sawyer, T. K.; Hadley, M. E. Melanotropins: Structural, Conformational and Biological Considerations in the Development of Superpotent and Superprolonged Analogs. *Pept. Protein Rev.* **1984**, *3*, 1–64.
(57) Sawyer, T. K.; Castrucci, A. M.; Staples, D. J.; Affholter, J. A.; DeVaux, A. E.; Hruby, V. J.; Hadley, M. E. Structure-Activity Relationships of [Nle^4, D-Phe^7]α-MSH: Discovery of a Tripeptidyl Agonist Exhibiting Sustained Bioactivity. *Ann. N. Y. Acad. Sci.* **1993**, *680*, 597–599.
(58) Haskell-Luevano, C.; Miwa, H.; Dickinson, C.; Hruby, V. J.; Yamada, T.; Gantz, I. Binding and cAMP Studies of Melanotropin Peptides with the Cloned Human Peripheral Melanocortin Receptor, hMC1R. *Biochem. Biophys. Res. Commun.* **1994**, *204*, 1137–1142.
(59) Rose, G. D.; Gierash, L. M.; Smith, J. A. Turns in Peptides and Proteins. *Adv. Protein Chem.* **1985**, *37*, 1–109.
(60) Momany, F. A.; McGuire, R. F.; Burgess, A. W.; Scheraga, H. A. Energy Parameters in Polypeptides. VII. Geometric Parameters, Partial Atomic Charges, Nonbonded Interactions, and Intrinsic Torsional Potentials for the Naturally Occurring Amino Acids. *J. Phys. Chem.* **1975**, *79*, 2361–2381.
(61) Némethy, G.; Pottle, M. S.; Scheraga, H. A. Energy Parameters in Polypeptides. 9. Updating of Geometrical Parameters, Nonbonded Interactions, and Hydrogen Bond Interactions for the Naturally Occurring Amino Acids. *J. Phys. Chem.* **1983**, *87*, 1883–1887.
(62) Dunfield, L. G.; Burgess, A. W.; Scheraga, H. A. Energy Parameters in Polypeptides. 8. Empirical Potential Energy Algorithm for the Conformational Analysis of Large Molecules. *J. Phys. Chem.* **1978**, *82*, 2609–2616.
(63) Nyburg, S. C. Some Uses of a Best Molecular Fit Routine. *Acta Crystallogr.* **1974**, *B30*, 251–253.
(64) Späth, H. *Cluster Dissection and Analysis. Theory, FORTRAN Programs, Examples*; Willey: New York, 1985; pp 16–32.
(65) Shizume, K.; Lerner, A. B.; Fitzpatrick, T. B. In Vitro Bioassay for the Melanocyte Stimulating Hormone. *Endocrinology* **1954**, *54*, 533–560.
(66) Goldman, J. M.; Hadley, M. E. Evidence for Separate Receptors for Melanophore Stimulation Hormone and Catecholamine Regulation of Cyclic AMP in the Control of Melanophore Responses. *Br. J. Pharmacol.* **1970**, *39*, 160–166.
(67) Vesely, D. L.; Hadley, M. E. Receptor-Specific Calcium Requirement for Melanophore-Stimulating Hormone. In *Pigment Cell: Unique Properties of Melanocytes*; Riley, V., Ed.; S. Karger: Basel, 1976; Vol. 3, pp 265–274.
(68) Wright, R. M.; Lerner, A. B. On the Movement of Pigment Granules in Frog Melanocytes. *Endocrinology* **1960**, *66*, 599–609.

JM9407264